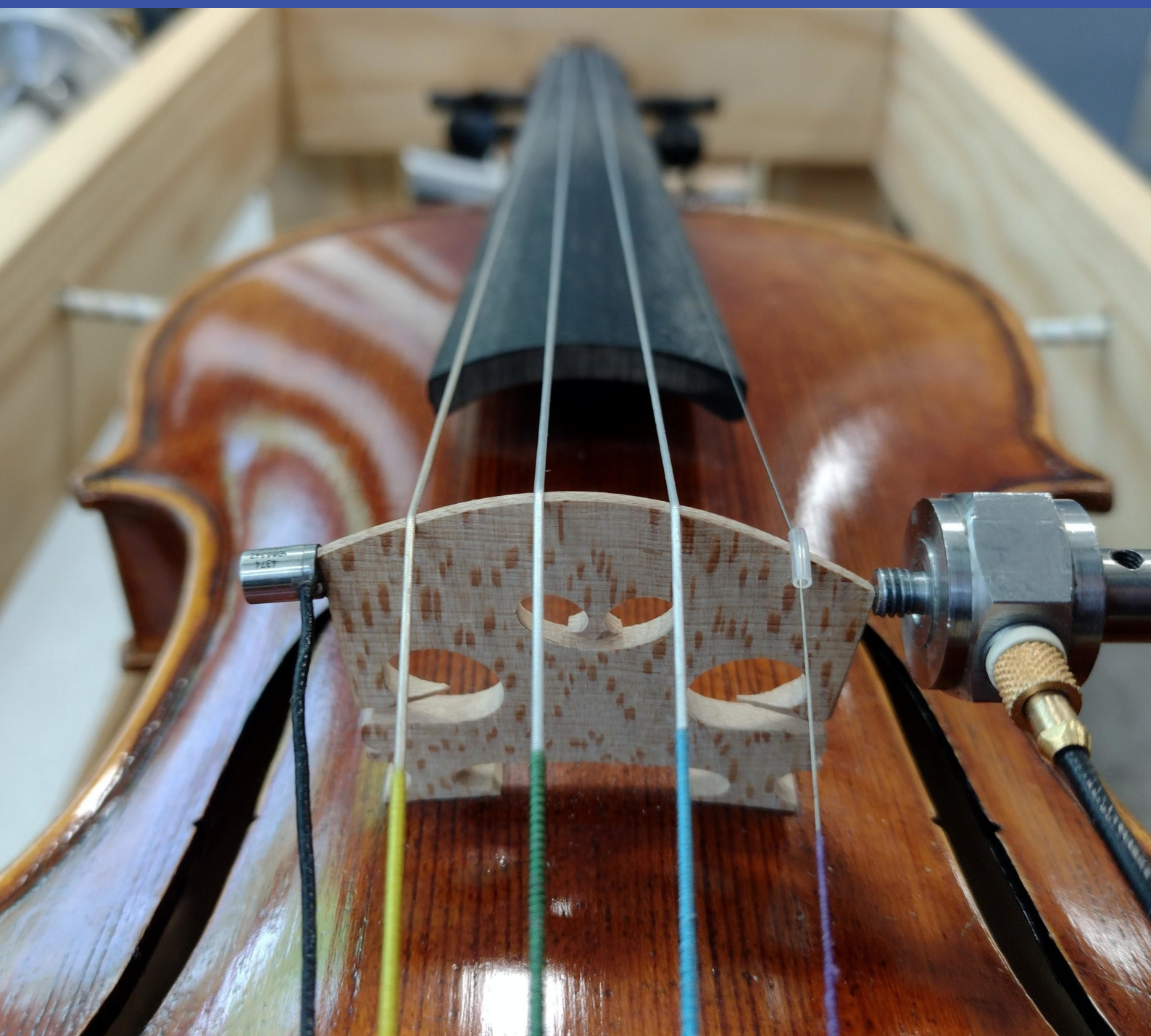


Practical Estimation of Violin Bridge Admittance

Master Thesis

Holger Rindel

July 10th, 2025



Practical Estimation of Violin Bridge Admittance

Master Thesis

July, 2025

By

Holger Rindel

Copyright: Reproduction of this publication in whole or in part must include the customary bibliographic citation, including author attribution, report title, etc.

Published by: DTU, Department of Electrical and Photonics Engineering, Ørsteds Plads, Building 352, 2800 Kgs. Lyngby Denmark
www.electro.dtu.dk

Preface

It is assumed that the reader has a basic knowledge in the areas of acoustics, signal processing and statistics.

This document is divided into a research paper as well as the thesis proper. The research paper is a condensed version of the thesis more suitable for scientific publication at a later date, e.g. as a JASA express letter.

Approval

This thesis has been prepared over five months at the Section for Acoustic Technology, Department of Electrical and Photonics Engineering, at the Technical University of Denmark, DTU, in partial fulfillment for the degree Master of Science in Engineering Acoustics, MSc Eng.

Holger Rindel - s194310

.....
Signature

.....
Date

Abstract

This thesis presents a practical and cost-effective method for measuring violin bridge admittance and radiativity, aiming to correlate mechanical-acoustic properties with perceived violin quality. Focusing on signature modes (A0, CBR, B1-, B1+), the study employs a pendulum for a predictable impulse excitation, with responses captured using a laser-Doppler vibrometer for admittance and a microphone for radiativity. Key aspects like string damping, excitation method, violin support, and mass-loading effects were investigated. Felt damping at the fingerboard's lower end and a stable wooden frame were found to give good results. The pendulum method achieved a level uncertainty of about ± 0.6 dB for the signature resonances. Strong correlations were found between admittance and radiativity for resonance frequencies and levels, and the computed transfer function between admittance and radiativity revealed a simple relationship between the two measures at low frequencies. This indicated that radiativity measurements can effectively replace the admittance for the purpose of investigating the signature resonances, reducing reliance on costly equipment. This accessible method advances violin research by working towards a standardized violin measurement method. A pilot study with eight violins failed to link perceived quality to measurable characteristics, highlighting the need for a robust quality assessment method with participants familiar with quality assessment.

Acknowledgements

I would like to thank my supervisors Jonas Brunskog and John Heebøll for their input and encouragement, and luthier Jørgen Skotte for his comments and especially the tour of his violin workshop.

I would also like to thank Jørgen and John for conducting the playing tests, and for providing most of the violins used for the project.

A great thanks to Henrik Hvidberg, whose assistance with constructing the pendulum was an essential part of the project.

List of Symbols

j	$\sqrt{-1}$
i, j	index (integer)
f	frequency (Hz)
f_0	natural frequency (Hz)
Δf	3 dB bandwidth (Hz)
Q	Q-factor = $Q = f_0/\Delta f$
ω	angular frequency (rad/s)
ω_0	natural angular frequency (rad/s)
k	stiffness (N/m)
m	mass (kg)
t	time (s)
G	gravitational acceleration ($\approx 9.8 \text{ m/s}^2$)
s^2	sample variance
μ	group mean / expected value
n	number of measurements
N	number of violins
R^2	squared correlation coefficient
$F(t)$	force (N)
$x(t)$	displacement (m)
$v(t)$	velocity (m/s)
$a(t)$	acceleration (m/s ²)
$Y(t)$	admittance (m/Ns)
$\underline{H}(\omega)$	generic transfer function
$\underline{H}_1(\omega)$	transfer function 1 for random excitation
$\underline{H}_2(\omega)$	transfer function 2 for random excitation
$\gamma(\omega)$	coherence $\gamma = \underline{H}_1(\omega)/\underline{H}_2(\omega)$
$\underline{F}(\omega)$	Fourier transform of $F(t)$
$\underline{V}(\omega)$	Fourier transform of $v(t)$
$\underline{A}(\omega)$	Fourier transform of $a(t)$
$\underline{U}(\omega)$	different instance of $\underline{V}(\omega)$
$\underline{Y}(\omega)$	Fourier transform of $Y(t)$
Notation	
$ \cdot $	absolute value (modulus)
ξ	sample mean of ξ_i
$\text{Var}(\cdot)$	variance
$E[\cdot]$	expected value (mean)
dB	decibel scale: $20 \times \log_{10}(\cdot)$

Signature Modes

A0	Helmholtz "Breathing" mode $f_{A0} \approx 280$ Hz
CBR	Center-Bout Rotation mode $f_{CBR} \approx 400$ Hz
B1-	First corpus bending mode $f_{B1-} \approx 460$ Hz
B1+	Second corpus bending mode $f_{B1+} \approx 530$ Hz

Abbreviations

DAQ	Data Acquisition
DOF	Degrees of Freedom
FFT	Fast-Fourier Transform
FRF	Frequency Response Function
IEPE	Integrated Electronics Piezo-Electric
LDV	Laser-Doppler Vibrometer
MEMS	Micro-Electro-Mechanical Systems
SD	Standard Deviation
SE	Standard Error (standard deviation of the sample mean)
SNR	Signal-to-Noise Ratio
SPI	Serial Peripheral Interface
SPL	Sound Pressure Level

Contents

Preface	ii
Abstract	iii
Acknowledgements	iv
List of Symbols	v
Paper	1
1 Background	7
1.1 Violin Acoustics	7
1.2 Violin Measurements	9
1.3 Violin Quality	9
2 Measurement Methodology	11
2.1 Common Setup	11
2.2 Equipment and Calibration	12
2.3 Validating measurement software	14
2.4 String Damping	15
2.5 Impact Hammer	19
2.6 Violin support	21
2.7 Sound Measurement	22
2.8 Arduino Sensors	23
3 Mass Loading	25
3.1 Mass-loading properties	26
3.2 Small Masses	28
4 Pendulum Excitation	29
4.1 Pendulum Method	29
4.2 Proof of concept	31
4.3 Designing the Pendulum	31
4.4 Final Pendulum	33
5 Pendulum Results	35
5.1 Measurement Setup and Playing Test	35
5.2 Quality Assessment Results	35
5.3 Measurement Results	36
5.4 Admittance/Radiativity transfer function	38
5.5 Quality Link	40
6 Discussion	42
7 Conclusion	44
Bibliography	45
A Additional Figures	47
B Pendulum Results	56

Practical Estimation of Violin Bridge Admittance

Abstract

This study presents a cost-effective method for measuring violin bridge admittance and radiativity, focusing on reliable estimation of the signature modes (A0, CBR, B1-, B1+). The importance of string damping, violin support, excitation method and mass-loading was investigated. Using a pendulum for impulse excitation, admittance and radiativity can be estimated. Results show strong correlations between admittance and radiativity for resonance frequencies and levels, suggesting that radiativity can partially substitute admittance measurements, reducing equipment cost significantly. A pilot study of perceived quality highlights the need for a standardized quality assessment method and participants trained in quality evaluation.

Introduction

An understanding of violin quality has long been desired, and multiple attempts have been made to link the perceived quality of the instrument to measurable characteristics. Bridge admittance Y is one of the most common ways of measuring the violin response, quantifying how an input force applied at the string notches causes the bridge, and by extension the instrument as a whole, to move [1]. Another common transfer function is the radiativity R of the instrument, relating input force to radiated sound. These two measures describe the interaction between instrument and player and are thought to contain the information necessary to predict perceived quality. The goal of this study is to develop a reliable and cost-effective method for obtaining the violin bridge admittance. This method is intended to be used for establishing links to perceived quality.

The signature modes of the violin appear as a collection of prominent resonances that dominate the low-frequency region of the frequency response functions, see Figure 1. Previous attempts have been made to link these modes to quality with varying success [2, 3]. These attempts were held back by a lack of robust, standardized methods for measurements and playing tests of the violins. An accessible and reliable measurement method as a standard is a much-needed step towards more conclusive findings

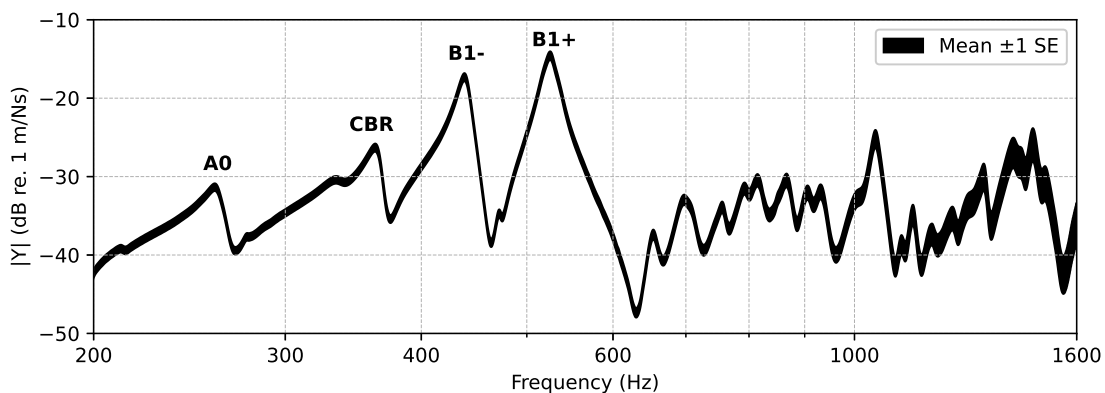


Figure 1: Bridge admittance results for a violin obtained with the final pendulum method. The width of the admittance curve indicates the sample mean ± 1 standard deviation of the sample mean (the standard error SE). The four signature resonances are clearly identifiable.

Methodology

For all measurement methods, the excitation was applied to the E-string corner of the bridge, while the response was captured at the G-string corner. A shaker was used for noise excitation and an impact hammer for impulse excitation. The responses were captured by either a laser-Doppler vibrometer, a piezoelectric accelerometer or a free-field microphone. The violins were tuned to standard A440 pitch to reflect playing conditions. Each set of measurements consisted of 10 measurements, where the violin was repositioned in its holding between measurements to more accurately represent the measurement uncertainty. When comparing different methods, measurements were alternated to account for variability from minor equipment repositioning or other unintended changes to the setup. Environmental factors were mitigated by only comparing measurements conducted on the same day. The importance of string damping, violin holding method, excitation method and microphone placement were investigated. The primary measurement method was iteratively refined based on these findings. The measurement and post-processing software was written in Python to make the method open-source <https://github.com/Hol-G/ViolinDTU2025.git>.

The viability of mass-loading sensors was investigated by comparing admittance measurements with different mass-loads attached to the bridge. The effective mass-loads were found by applying a simple correction to the admittance results, aligning the B1+ resonance frequencies for the free and loaded admittance.

Pendulum Design

A pendulum was developed to deliver a consistent impulse to the bridge for each impact. The design was the result of multiple iterations, aiming to make the impulses as similar as possible for different violins. The pendulum force spectrum was estimated using a "true" admittance (from impact hammer measurements) and the velocity response to the pendulum excitation. The pendulum impulse was estimated using three representative violins, with the final force spectrum estimate being a smoothed average. This resulted in a pendulum force spectrum that could be used as weighting curve for the response spectrum of any violin, capable of giving the admittance or radiativity depending on the measured response. The uncertainty of this estimate was also determined.



Figure 2: Picture of the radiativity measurement setup, with the pendulum striking the E-string corner of the bridge and a microphone placed to capture the sound pressure at the G-string corner. Felt for string damping can be seen for both the upper and lower string lengths.

Final method

The pendulum was used for bridge admittance and radiativity measurements for eight violins. The resonance frequency, peak level and Q-factor were extracted for the signature modes A0, CBR, B1- and B1+. A simple playing test was also conducted to better understand the challenges that arise when attempting to link measurement results to quality ratings.

Results

String damping proved to be important, with different materials and positions having significant influence over the measured admittance. It was found that the damping material should not be placed at the upper end of the fingerboard, with a piece of felt at the lower end of the fingerboard giving the best results. When using an impact hammer, it was determined that the mass of the hammer should be very low and that the tip should be hard. Otherwise, the duration of impact will be too long and the admittance results inaccurate. The choice of violin support was found to have some influence, but the difference between holding methods is small compared to the effect of holding the violin for playing. A safe and reliable holding method with a simple wooden frame was favored over free-free boundary conditions.

A radiativity measurement conducted adjacent to the G-string corner of the bridge was found to yield relevant results while not requiring room acoustics tailored to the measurement, see Figure 2. An attempt was made to use modular sensors with an Arduino microcontroller to serve as cheap alternatives to professional equipment, but they were not suited for accurate measurements. Even lightweight sensors were found to have a noticeable mass-loading effect on the admittance, shifting the signature resonances. Attempts to link quality assessments to measured values did not succeed due to the unreliability of the quality assessment.

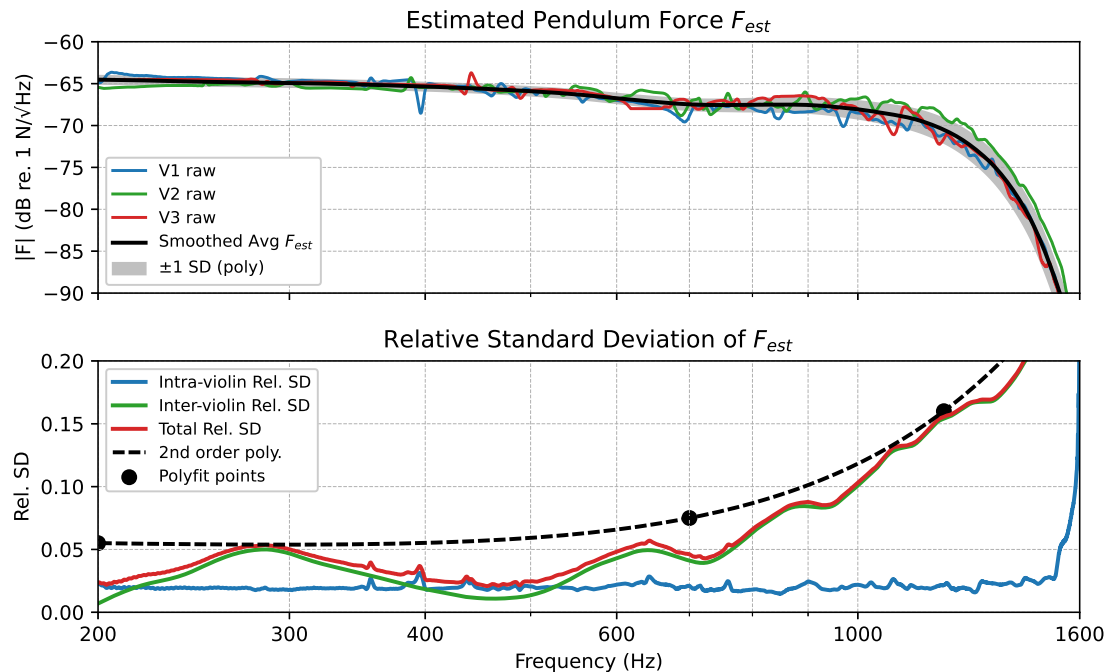


Figure 3: Top: Estimates of pendulum force spectrum for each of the three test violins, as well as the averaged smoothed estimate with a shaded area of ± 1 standard deviation (SD). Bottom: Intra- and inter-violin relative standard deviations as well as combined relative standard deviation with a polynomial fit as an envelope.

Pendulum

The uncertainty of the force spectrum estimate is the combination of both the intra-violin uncertainty and the inter-violin uncertainty. It was found that as the pendulum mass decreases the force spectrum becomes flatter and the difference between violins decreases. Due to measurement uncertainty and fundamental differences between impact hammer and pendulum excitation, the force spectrum estimates required smoothing to be realistic, see Figure 3. It was found that the inter-violin variability dominates the uncertainty of the force spectrum estimate, but still allows the pendulum method to measure an accurate bridge admittance with a standard deviation of about ± 0.6 dB for the signature resonances. Due to the smoothness of a short impulse, this uncertainty does not affect resonance frequency and Q-factor significantly.

Admittance and Radiativity

Significant correlation between the admittance and radiativity measurements was found for the signature resonance parameters: *frequency*, *level* and *Q-factor*. While non-linear effects were indicated, this led to the idea that there exists a simple transfer function. The transfer function between admittance and radiativity was computed for all violins, and shifted to align the A0 frequencies. The relationship was nearly the same for all the violins, and a running average was computed, see Figure 4. Applying this transfer function to the radiativity results was found to give reasonable estimates for the admittance for the B1 signature resonances. Given the overlap in information for admittance and radiativity, it was concluded that the radiativity at the G-string corner of the bridge can function as a reasonable replacement to the bridge admittance.

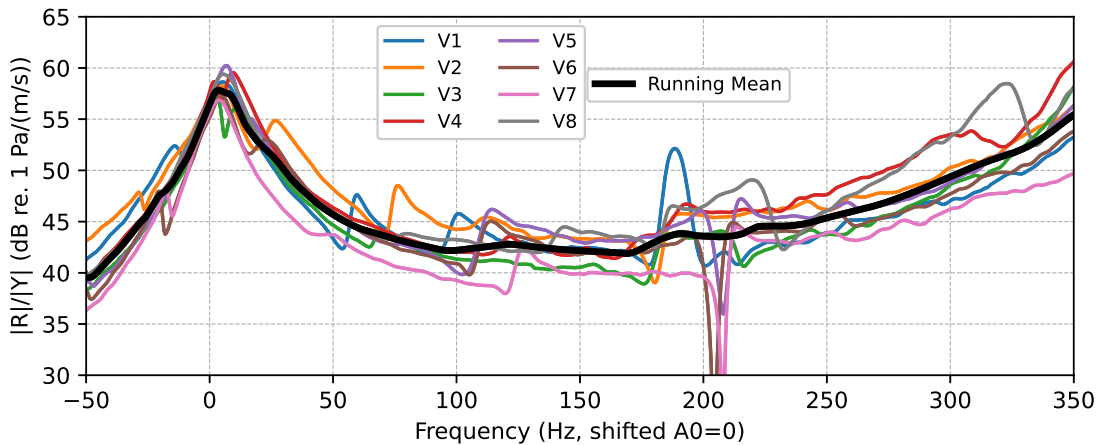


Figure 4: Transfer functions between admittance Y and radiativity R for the 8 violins, with a running mean. Frequency axis aligned with the A0 frequency for the radiativity measurement.

Discussion

The pendulum method has been demonstrated to function as a viable replacement to impact hammers, and has great potential for wider use. An even lighter pendulum could further improve the accuracy of the method. Replacing the bridge admittance measurement with a radiativity measurement would greatly decrease the cost of the equipment necessary to investigate the signature resonances. The relationship between the bridge admittance and radiativity would be worth investigating further, perhaps extending the relationship to higher frequencies.

The largest hindrance to establishing links between measurements and perceived quality is the robustness of the quality assessments. It is proposed that a standardized method should be developed, specifying room acoustics, quality descriptors [4] and playing tasks. The participants should also be trained in the skill of assessing violin quality.

Conclusion

The practical aspects of measuring violin frequency response functions have been investigated, demonstrating the importance of string damping, excitation method, mass-loading and violin support. A very simple method has been developed for obtaining admittance and radiativity measurements for the violin bridge using a simple pendulum, both of which can be used to obtain the signature resonances. It has been shown that a radiativity measurement at the bridge can effectively replace the admittance measurement for investigating signature resonances, greatly improving the affordability of violin measurements.

References

- [1] Woodhouse J. "The acoustics of the violin: a review". In: *Rep. Prog. Phys.* 77 (2014).
- [2] Saitis C., Fritz C., Giordano B., and Scavone G. "Bridge admittance measurements of 10 preference-rated violins". In: *Acoustics 2012, Apr 2012, Nantes, France.* (2012).
- [3] Bissinger G. "Structural acoustics of good and bad violins". In: *J. Acoust. Soc. Am.* 124(3) (2008), pp. 1764–1773.
- [4] Fritz C., Blackwell A. F., Cross I., Woodhouse J., and Moore B. C. J. "Exploring violin sound quality: Investigating English timbre descriptors and correlating resynthesized acoustical modifications with perceptual properties". In: *J. Acoust. Soc. Am.* 131(1) (2012), pp. 783–794.

Chapter 1 Background

This thesis is the third project investigating violins at the DTU Vibrolab. The two previous projects utilized a shaker and laser-Doppler vibrometer (LDV) for obtaining the admittance from one corner of the violin bridge to the other. In 2023, Flocken [5] used bridge admittance measurements and playing tests to determine whether a prolonged vibration of the instrument leads to perceptible and measurable changes. No significant differences were found, and the measurable differences could have been caused by environmental changes. Then in 2024, Benson [6] investigated the effect of humidity on the bridge admittance, finding that humidity can shift the frequencies of resonance peaks by up to 8%.

The goal of this thesis is to develop a method that can obtain the bridge admittance of the violin reliably, while not being prohibitively expensive. An affordable method would make violin measurements more accessible to luthiers and educational institutions alike, potentially increasing participation in violin research. The intended use of this method is to establish a link between the quantifiable mechanical-acoustic properties and the perceived quality of violins from the perspective of the player.

1.1 Violin Acoustics

The violin is a wooden box that transforms the action of bowing the strings into radiated sound. A simple illustration of the instrument can be seen Figure 1.1. The process of generating sound can be simplified in the following manner [1]:

1. Bowing causes the strings to oscillate.
2. The strings apply a varying force to the bridge at the string notches, predominantly side-to-side.
3. The vibrations are transmitted through the bridge, which connects to the top plate of the violin at two feet. These vibrations are transmitted to the rest of the instrument, especially through the soundpost, which connects the top and back plates of the violin.
4. The motion of the different parts of the violin radiate sound.

The strings of the violin are always in tension, and are an integral part of the structure, meaning that tuning each of the strings changes the mechanical properties of the entire instrument. Bowing results in a "stick-slip" excitation of the string, with the applied force taking the form of a sawtooth wave. It is assumed that the violin bridge represents the main interaction between the strings and the body. This interaction can be understood by examining the frequency response functions (FRFs) at the string notches of the bridge, resulting in a 3-dimensional transfer function for each of the four string notches.

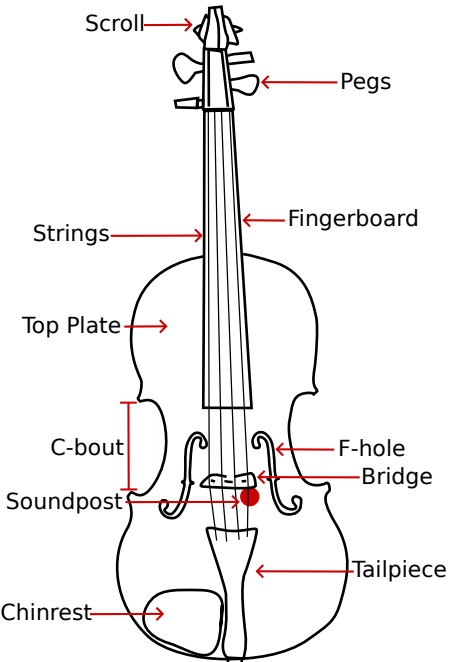


Figure 1.1: Drawing of a top-down view of a violin, labeled with names of main parts.

The mechanical transfer function between force F and velocity v is called admittance Y , while the transfer function between force and sound pressure p is called radiativity R :

$$\text{Admittance: } Y = \frac{v}{F} \quad \text{Radiativity: } R = \frac{p}{F} \quad (1.1)$$

The "bridge admittance" is usually measured as a single transfer function, relating the force input at one corner of the bridge to the velocity response at the opposite corner. An example bridge admittance using impact excitation can be seen in Figure 1.2.

The admittance of the bridge goes both ways, such that the vibrations of the violin body feed back into the strings and is thus felt by the player through the bow. The experience of the violinist therefore consists not only of the emitted sound, but also the feedback felt when bowing the strings. This is what is meant by *playability*, and is thus directly linked to the bridge admittance.

The body vibrations can be described by its modal contributions. At low frequencies, the violin is characterized by individual modes, while at higher frequencies it makes more sense to discuss statistical effects due to the increasing modal overlap. A number of low frequency modes are often referred to as *signature modes*, and are prime candidates for comparing different violins, on account of them being easily identified in the FRFs of most violins [3]. This thesis focuses on the following four signature modes:

- **A0:** Helmholtz-type cavity mode, "breathing" through the f-holes.
- **CBR:** Center Bout Rotation.
- **B1- and B1+:** Combined breathing/bending modes

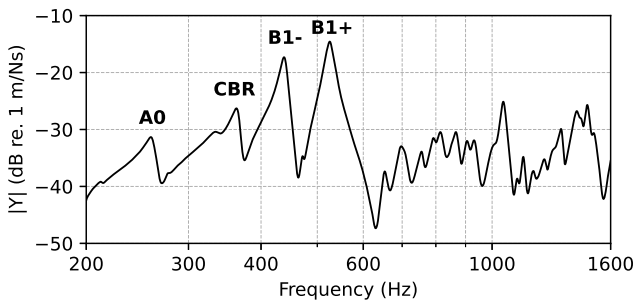


Figure 1.2: Example bridge admittance, with signature resonances labeled (Violin V5, using pendulum method).

The A0, B1-, B1+ modes are strong radiators, and are therefore very relevant to sound radiation. The CBR mode is also of interest since it is often quite prominent, and is coupled to breathing modes due to the off-center position of the soundpost. In fact, it is this placement of the soundpost which allows the bowed strings to excite the three strongly radiating modes by breaking up the left-right symmetry of the violin. This coupling of the strongly radiating modes is of particular interest, since the soundpost position is one of the few parts of the violin which can be adjusted after its completion. The modes can be seen as resonance peaks on the transfer functions, and can be described by three numbers: Frequency, Magnitude and Q-factor. The Q-factor indicates the sharpness of the resonance peak, and is calculated as the resonance frequency f_0 divided by the 3 dB bandwidth Δf , reflecting the mode's energy dissipation.

At high frequencies, the violin displays complicated behavior, with the envelope of the response showing clear "humps", not unlike the formants of human speech. This is in contrast to other stringed instruments like the guitar, which do not have a formant-like behavior at high frequencies [1]. For the violin, the most prominent high frequency feature is a very large hump around 2-3 kHz that is often called the "bridge hill", and is thought to be very important for violin quality [7]. While undoubtedly relevant, these high frequency features are not investigated in this thesis, which focuses on the signature modes.

1.2 Violin Measurements

Ideally, the admittance of the bridge would be obtained by bowing the strings and measuring the input admittance at each string notch, but this is not practical. Instead, the admittance of the violin bridge is usually measured by tapping one corner of the bridge with a hammer and measuring the velocity at the opposite corner with an LDV. This corner-to-corner admittance captures the main bowing direction, but fails to account for the other two dimensions of motion and doesn't distinguish between the string notches. Technically, this measurement gives the transfer admittance from corner to corner rather than the input admittance, but for low frequencies the bridge can be assumed to be rigid and the transfer admittance will be similar to the input admittance.

It has been shown on a cello (which is similar to a violin except in size) that excitation by bowing is not fundamentally different from impact excitation and that the corner-to-corner admittance is a good approximation for all four strings [8]. While the bridge can also be excited by a shaker (as in [5] and [6]), the impact hammer is preferred since it does not couple mass to the bridge and gives more consistent results because mass loading conditions do not change between measurement sessions [9]. This mass-loading problem also applies if an accelerometer is used instead of a laser for the response measurements.

While the unbowed strings are free to vibrate when playing, they are usually damped when measuring admittance and radiativity. This is done to prevent string resonances from obscuring the body resonances. Even though it is quite important for the robustness of bridge admittance measurements, no standardized string damping method exists. The holding of the violin is another challenge. Methods such as clamping the neck, suspending the instrument from rubber bands or using a violin stand give different results [10]. Holding the violin for playing could be considered more accurate, but that is not a practical solution since the holding conditions must be reproducible in order for the measurements to be useful.

Another way of investigating the body modes of the violin is with laser scans of multiple positions from which a great number of transfer admittances can be computed [3]. This gives detailed information about the mode shapes, but lacks the simplicity of the corner-corner measurement. The radiativity is also difficult to measure properly since sound radiation is distance dependent, directional and affected by room acoustics.

Violin measurements are further complicated by environmental factors, which have significant influence [6]. Even small changes in relative humidity can cause admittance changes that are much larger than measurement uncertainty [11]. Even a 1 gram change to the water weight of the violin can be enough to cause significant changes to the B1- mode. For this reason, it is important that environmental changes are considered carefully when comparing measurements.

1.3 Violin Quality

Perhaps the most extensive study on violin quality was performed in 1991 by Dünnwald [12]. Hundreds of violins were excited by a sinusoidal force at the bridge, and the radiated sound measured in the far-field. It was found that the A0 mode should be loud, and other quality parameters were extracted based on the sound content in different frequency ranges, relating the different bands to terms such as *nasality*, *brilliance* and *clarity*. Unfortunately, it lacks details on the choice of bands or how the quality assessment of the violins was conducted.

Multiple further attempts have been made to relate the measured response of violins to their perceived quality, often using a unipolar scale from "bad" to "excellent". Bissinger [3] performed admittance and radiation measurements of 17 violins, finding that the A0 radiativity is higher and the radiativity profiles more "even" for excellent violins. No other quality link was found, and it was pointed out that the robustness of the quality assessments is a large hindrance. Similarly,

Saitis et al. [2] measured the bridge admittance for 10 violins that had been rated in preference by 13 participants in a carefully controlled environment. Again, no clear link between admittance and quality was found.

Since the reliability of the playing tests is a big limitation, Fritz et al. [4] investigated the verbal descriptors commonly used for violin quality, clustering words used to convey a similar meaning. For overall sound quality, it was concluded that the terms made up a 3-dimensional space, with two of the dimensions appearing to carry judgment of whether a violin is good or bad. This mapping of quality descriptors is a good reference for designing playing tests and will be used in this thesis. It was then attempted to relate some of the terms to artificially modified violin sounds in a perceptive study. The findings were mostly inconsistent with the findings of Dünnwald, and found that there was disagreement between the participants on what constituted a "good" and "nasal".

Chapter 2 Measurement Methodology

In this chapter, the methods for measuring the violin are investigated using the primary test violin V1. An iterative approach was used, gradually improving the primary measurement method.

2.1 Common Setup

Here follows the general measurement method used throughout the thesis, irrespective of excitation method or the measured response. Figure 2.1 shows some of the measurement setup.

The strings were tuned to standard A440 pitch for all measurements, ensuring tension consistent with playing conditions. The strings were damped in two places to eliminate the string resonances from the frequency response functions: A large piece of felt was placed at the edge of the fingerboard to eliminate the main string resonances, while a smaller piece of felt was placed to dampen the string lengths between the bridge and tailpiece. This choice of damping method is based on the findings in Section 2.4.

All measurements were performed by exciting the E-string corner of the bridge and measuring the response at the G-string corner. This direction was chosen since the G-string side usually has a wider and flatter surface on which to attach a sensor. Note that most of the literature uses the opposite direction, but due to reciprocity the chosen direction should not matter. The violin was placed horizontally in a wooden frame, resting the lower bout on two shoulder rest feet, while the neck rested on a length of cord, approximating the contact points of the player (see Section 2.6). The constant pressure applied to the chin rest when playing was not accounted for.

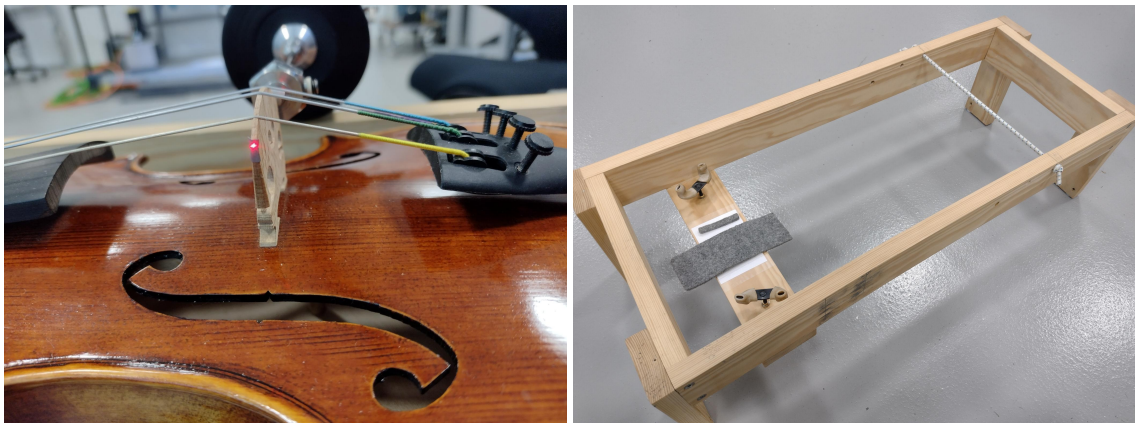


Figure 2.1: Left: Laser dot pointed at the G-string corner of the bridge. Right: Violin frame.

For all measurements, a sample rate of 3200 Hz was used with an FFT size of 6400. This gave results with a bandwidth of 1600 Hz and a frequency resolution of 0.5 Hz, which is well suited for investigating the signature resonances (200-600 Hz). The equipment was calibrated for each measurement session.

The measured frequency responses were averaged across 10 measurements to account for measurement uncertainty stemming from both equipment positioning and signal noise. The violin was replaced in the frame between each measurement. In order to avoid drift due to equipment changes, all measurement comparisons were based on alternating between the different configurations. When comparing measurements, it was essential that all measurements were conducted in a single session in order to minimize calibration error and environmental effects.

2.2 Equipment and Calibration

The initial measurement setup was inherited from the previous projects [5, 6], and used a B&K Pulse type 3560 FFT Analyzer along with the proprietary PULSE software that ran on the laboratory computer. This was updated to use a Focusrite Scarlett 2i2 soundcard connected to a laptop using Python for signal processing. This was done to make the measurement software open source and to have more control over the measurement procedure and signal processing. The results of this migration from PULSE to Python are discussed in Section 2.3, and the code can be found at <https://github.com/Hol-G/ViolinDTU2025.git>.

2.2.1 Excitation Methods

Both noise and impact excitation were used. Note that the sensitivity of some transducers had to be adjusted depending on the excitation method in order to avoid signal overload.

- **Noise:**

A shaker mounted on a tripod excites the bridge with white noise. A drive rod connects to a force transducer which pushes against the E-string corner of the bridge. Welch's method was used with 90% overlapping segments and the Hanning window. The auto- and cross-spectra were averaged across 100 segments, from which the transfer functions $\underline{H}_1(\omega)$, $\underline{H}_2(\omega)$ and the coherence $\gamma^2(\omega)$ were obtained. In this paper the $\underline{H}_1(\omega)$ transfer function was used.

- **Impact:**

An impact hammer/pendulum strikes the E-string corner of the bridge. The transfer function $\underline{H}(\omega)$ was computed for each impact and averaged across 10 impacts. The onset of the impact was detected by the response signal exceeding a set value, which was adjusted as needed. A 0.5 s rectangular window starting 0.05 s before the onset was used to capture the violin response. A rectangular window is sufficient since the signal before and after the impact is close to zero. Impact excitation is further investigated in Section 2.5.

2.2.2 Bridge Response

The mechanical bridge response was measured either with an LDV or a piezoelectric accelerometer. Since both of these sensors are directional and the edge of the bridge is not perfectly vertical when the violin is placed in the frame, they measure slightly different transfer admittances. Some testing found that the accelerometer gives a slightly larger velocity response than the laser for frequencies below 1 kHz, but otherwise the admittance was unchanged. A sound measurement was introduced to obtain the radiativity of the violin.

- **Velocity:**

The velocity was measured using an LDV pointed at the G-string corner of the bridge. A piece of reflective tape was attached to get a good signal. A signal delay of 1.221 ms had to be accounted for when performing 2-channel measurements in order to obtain accurate phase results.

- **Acceleration:**

A piezoelectric accelerometer was attached to the G-string corner of the bridge using beeswax. The acceleration spectrum was converted to velocity by $\underline{V} = \frac{1}{j\omega} \underline{A}$. While this sensor was preferred for much of the project on account of having less signal noise, it was ultimately less reliable due to the difficulty of attaching it to the bridge and had a mass-loading effect which could not be ignored, see Chapter 3.

- **Sound Pressure:**

A GRAS 46AE 1/2" free-field microphone was placed about 5 mm from the G-string corner of the bridge, allowing room to maneuver the violin. This proximity to the source ensured a good SNR despite not using an anechoic chamber. See Section 2.7 for more.

It was also attempted to conduct acceleration and sound pressure measurements using cheap sensors connected to an Arduino Nano V3, but these did not give usable results (Section 2.8).

2.2.3 Equipment Overview

The B&K force transducer and piezoelectric accelerometer were run through an amplifier before connecting to a soundcard. The LDV was connected directly to the soundcard, while the microphone was connected to a separate data acquisition device.

Miscellaneous

- Soft felt for string damping.
Thickness: 4 mm, Density: 0.2 g/cm³
- Large: 135×50 mm and small: 8×50 mm
- Wooden Frame
- Tripod
- Beeswax
- Reflective tape

Signal Processing

- Exciter amplifier (for the shaker)
- FFT Analyzer
(B&K Pulse 3560-B-130)
- Conditioning amplifier (Nexus 2692)
- Focusrite Scarlett 2i2 soundcard
- ROGA Instruments IEPE DAQ
(Plug.n.DAQ Lite)

Excitation and Response

- Shaker (B&K 4810)
- Piezoelectric accelerometer (B&K 4344)
- Laser-Doppler vibrometer (Polytech PDV-100)
- Force transducer (B&K 8200)
- Impact hammer + tips (B&K 8202)
- Free-field microphone set (GRAS 46AE)
- Pendulum

Calibration

- Calibrator (B&K 4294)
- Microphone calibrator (GRAS 42AG)
- Mass ≈ 105 g

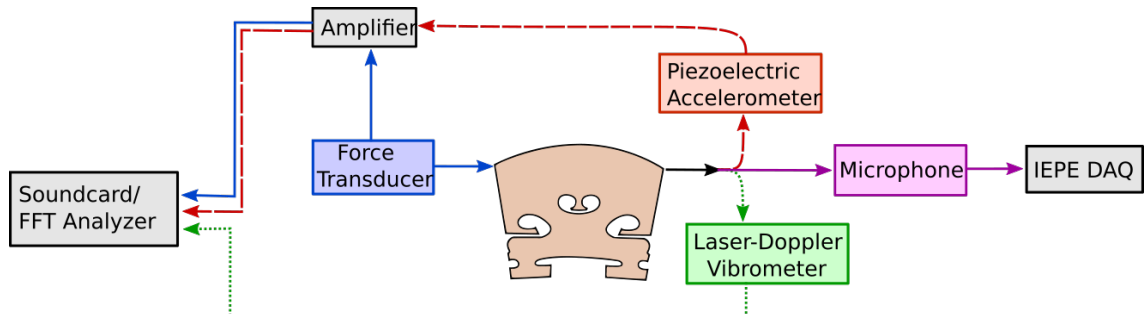


Figure 2.2: Basic overview of equipment connections for admittance and radiativity measurements.

2.2.4 Calibration

First, the piezoelectric accelerometer is attached to a calibrator using beeswax. The gain is adjusted to achieve the desired RMS of 10 m/s² at 159 Hz.

The force transducer is mounted on a shaker with a known mass and the accelerometer on top. Newton's 1st law can then be applied, whereby $F/a = m$ is obtained as the desired transfer function. The total mass m was measured to be 108.5 grams, which includes the accelerometer mass and transducer top mass of 3 grams [13]. The LDV is pointed at the accelerometer that is mounted on the shaker. The desired transfer function between velocities is simply 1. The GRAS 46AE microphone is calibrated using the GRAS 42AG calibrator at 94 dB SPL and 1000 Hz.

2.3 Validating measurement software

The validity of the soundcard/Python measurement was validated by comparing results with the original measurement arrangement. The undamped violin was excited by a shaker and the response measured by the piezoelectric accelerometer. The only changes between measurements were the cable connections as shown in Figure 2.2, ensuring that any differences could be fully attributed to the hardware and/or software. This comparison also served as a test for the calibration implementation in Python.

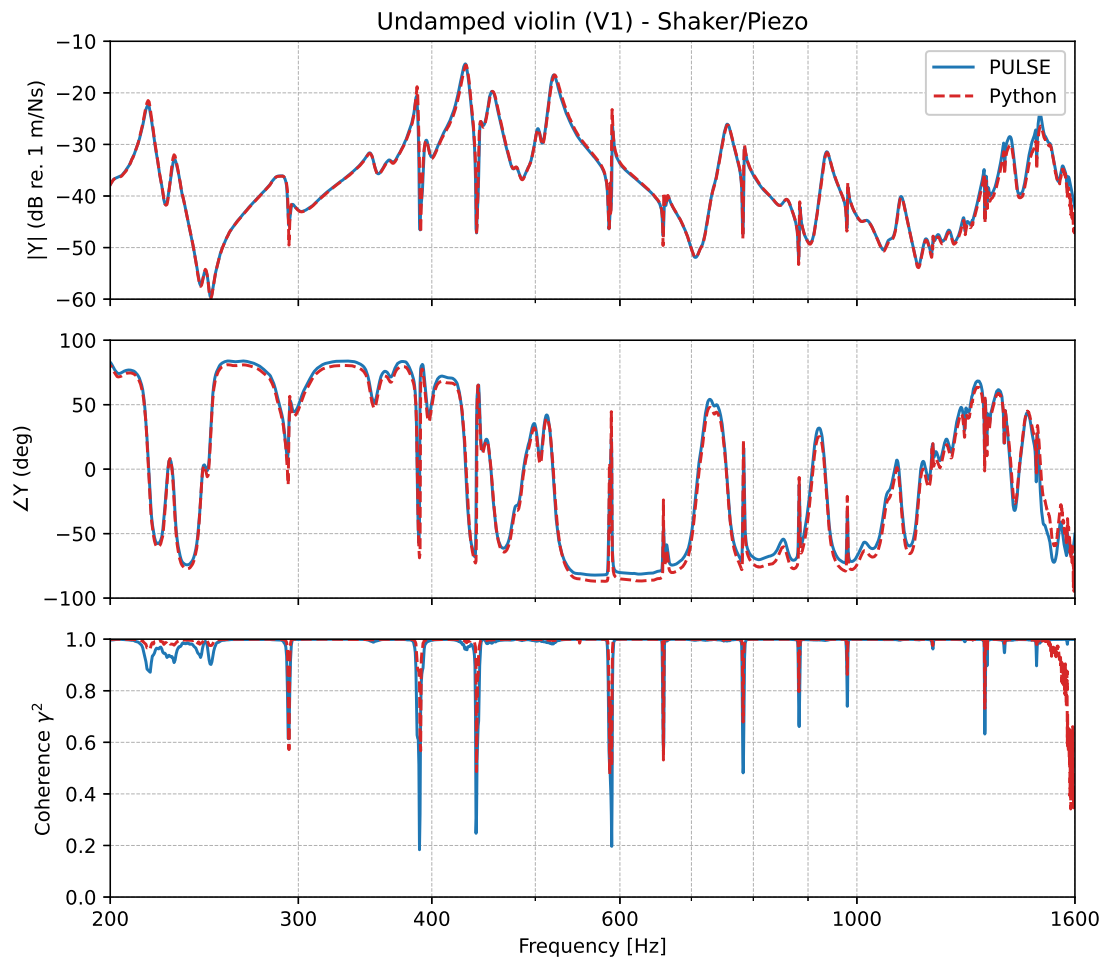


Figure 2.3: Admittance magnitude, phase and coherence for both old and new measurement systems.

The H_1 magnitude and phase, as well as the coherence for both systems are presented in Figure 2.3. The magnitudes are very consistent, validating the calibration procedure. Minor differences are observed for phase and coherence, with the most notable discrepancy being a high frequency roll-off of the coherence for the Python system. This is attributed to the practical limitations of the sample rate, where the Nyquist frequency of half the sample rate is not a realistic frequency cut-off. This could be mitigated by oversampling, but this was not implemented due to being unnecessary for investigating the signature resonances.

Since the discrepancies appear to stem from differences between the B&K FFT Analyzer and the soundcard, the Python implementation is accepted as a replacement. Note that the resonances below 250 Hz stem from the shaker mounting, not the violin.

2.4 String Damping

Why damp the strings? This is not done when playing the violin, so it might not be obvious why this is necessary.

The strings are damped because the string resonances do not provide useful information about what makes each violin unique. With a standard A440 tuning, the frequencies of the string resonances are completely predictable. The large dips in coherence seen in Figure 2.3 are the string resonances, and their effect on the bridge admittance is significant. When a string resonance is close to a body resonance, it becomes impossible to accurately determine the frequency and level of the body resonance.

2.4.1 Previous Methods

In the course of the literature study for this project, it became clear that no standard for string damping exists. This is an oversight, since it prevents measurements from being directly comparable.

Many methods have been used to achieve string damping: Plastic cards, business cards, folded tissue, foam and nylon ribbons to name just a few. It has been noted that the position of the damping material can noticeably affect the measurement results [14]. It has also been stated that "the requirement for adequate damping is that no musical pitch can be heard when the strings are plucked" [8], but it will be demonstrated that this is an insufficient criterion.

This thesis will therefore endeavor to determine a reliable string damping method, which can be used as a standard henceforth. A number of different string damping methods were tested and the best chosen.

2.4.2 Setup

The idea with string damping is to remove the string resonances from the admittance while changing the rest of the admittance as little as possible. Criteria are established to judge the different string damping methods:

1. The string resonances should be eliminated from the admittance. A necessary, but insufficient criterion is that the resulting coherence dip must be removed.
2. The damping material must not significantly change the admittance outside the string resonances.
3. The placement of damping material should be reliable and unambiguous. The material should be widely available.

Many preliminary investigations were made using the B&K PULSE system, testing different materials and positions. Of these, it was determined that the best damping method was to place two pieces of paper tower along the fingerboard of the violin. This method was used as a reference to which the other methods could be compared.

Some obvious limitations became apparent during the preliminary testing. The damping material should be sufficiently stiff to restrict string movement and should not be placed too close to the bridge, since that will cause a mass-loading effect.

All damping materials were woven between the strings, passing under the D and A strings, and were placed in one of three ways: Aligned with the lower end of the fingerboard, aligned 1 inch from the upper end of the fingerboard or aligned with the edge of the violin body.

The two materials chosen for in-depth investigation were some soft felt and standard playing cards. A piece of felt was placed either along the string length, ensuring maximum contact area, or placed across the strings with a smaller contact area. Stacks of 5 and 10 playing cards were

used. Pictures of the damping methods can be seen in Figure A.1 in the appendix. The different damping methods are listed below:

- | | |
|---------------------------------------|---|
| (a) Felt along lower fingerboard | (f) 10 playing cards at lower fingerboard |
| (b) Felt along upper fingerboard | (g) 10 playing cards at upper fingerboard |
| (c) Felt across lower fingerboard | (h) 5 playing cards at lower fingerboard |
| (d) Felt across middle of fingerboard | (i) 5 playing cards at upper fingerboard |
| (e) Felt across upper fingerboard | (j) 2 layers of paper towel |

2.4.3 Results

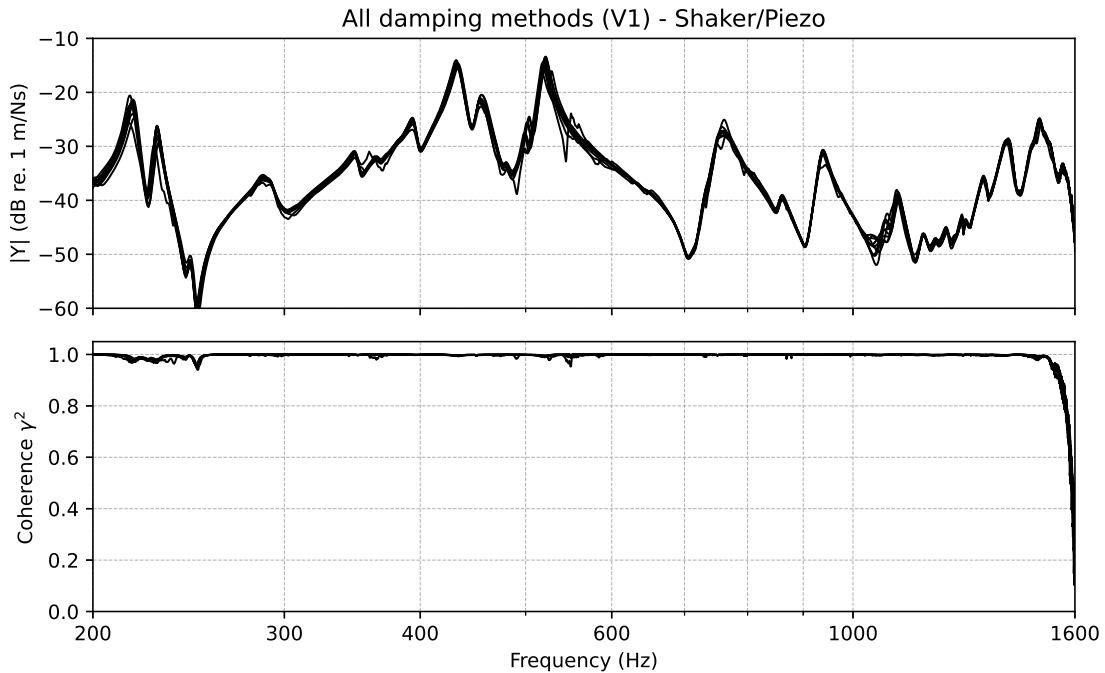


Figure 2.4: Admittance magnitude and coherence for all damping methods.

The results for all the damping methods are seen on Figure 2.4. All the damping methods prevented any musical pitch from being heard when plucking the strings, and they all resulted in much improved coherence. However, significant variation for the magnitude of the admittance can be seen.

Placing the damping material only on the upper end of the fingerboard resulted in very bad results regardless of material. Each of the three damping methods shown in Figure 2.5 (left) resulted in jagged admittance curves at one or multiple places. It is suspected that if only the upper segments of the strings are damped, most of the string lengths are still free to disturb the admittance.

An example highlighting the importance of placement can be seen on Figure 2.5 (right). The B1+ resonance is shown for the stacks of 5 and 10 playing cards in the same two positions. It is clear that position is just as important as material. None of these damping methods were desirable, giving inconsistent results at the very important B1+ resonance.

All the playing card configurations resulted in admittance curves that deviated significantly from the undamped admittance. For configuration (a) and (b), where the piece of felt was placed along

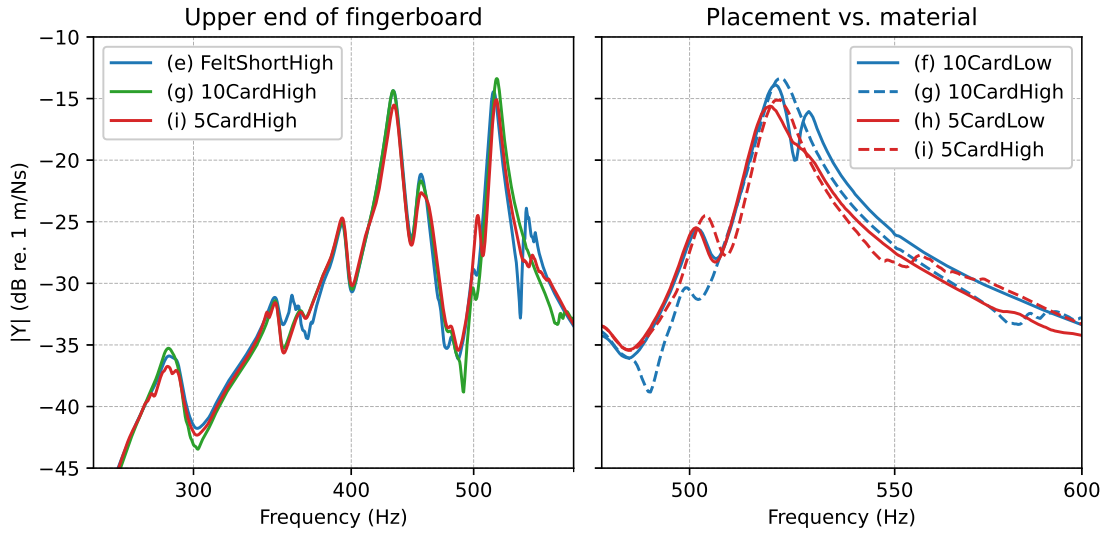


Figure 2.5: Bridge admittance for different damping methods. Left: Different materials with similar placement. Right: Two materials in two positions.

the string length, the B1+ mode was excessively damped. That left out configurations (c), (d) and (j) as the best options, but (d) had much larger measurement uncertainty than the other two. The two best methods were thus: the felt placed across the lower end of the fingerboard, and the paper towel from the preliminary measurements. While the results for the paper towel method had a slightly smaller uncertainty, the felt resulted in a more accurate FRF around both of the B1 modes, and caused slightly less damping of the peaks.

Therefore (c) was chosen as the best method, and was used for all other measurements in this thesis. This damping method also managed a coherence above 0.99 for the entire range from 250 to 1400 Hz.

Figure 2.6 shows the admittance of the damped and undamped violin. It can be seen that the chosen damping method results in a smooth FRF, which is in good agreement with the undamped response (except at the string resonances of course). Note that the resonances around 390 and 430 Hz were greatly disturbed by the string resonances. The A0 resonance around 287 Hz was affected in level and, while difficult to see, the B1+ resonance around 520 Hz was shifted slightly down in frequency by the string resonance at 588 Hz. The uncertainties for the two measurement sets are very similar, meaning that the placement of the damping material adds very little uncertainty.

2.4.4 Lower string damping

For later measurements of violin V3, it turned out that the lower string sections between the bridge and tailpiece were responsible for noticeable string resonances at high frequencies >1000 Hz. Therefore, a small piece of felt was placed at the tailpiece, woven between the strings. This final damping method can be seen in Figure 2.7.

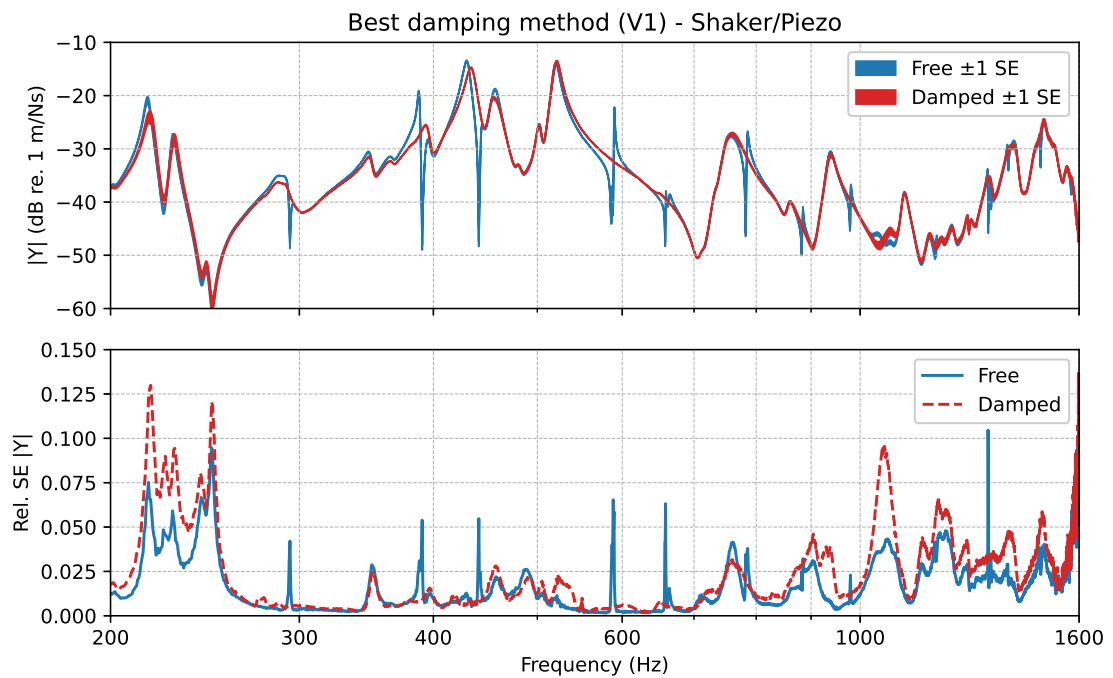


Figure 2.6: Top: Admittance magnitude for the undamped and damped strings with the width of the curves indicating the mean ± 1 standard deviation of the mean (the standard error SE). Bottom: The relative standard error.



Figure 2.7: Final damping method with a large piece of felt at the edge of the fingerboard and a smaller piece of felt woven between the strings near the tailpiece.

2.5 Impact Hammer

The initial measurement method used for the investigation of string damping excited the bridge with a shaker. While effective at exciting a broad frequency range using white noise, the coupled mass affects the FRF significantly. An impact hammer by contrast, offers an excitation method with negligible mass-loading due to its very short contact time.

To accurately measure the FRF, the impact hammer must excite a broad range of frequencies at an evenly high amplitude. A flat excitation spectrum is important to ensure that the response reflects the violin's properties rather than the variations in the input force. An uneven spectrum can lead to problems with bad SNR and inadequate excitation at some frequencies.

The ideal impact is infinitely short, resulting in a perfectly flat spectrum. For a given sample rate, as long as the duration is less than one sample (and is contained within a single sample), the spectrum will be completely flat. The impact can naively be modeled as a 1-DOF mass-spring system, with an initial velocity $\dot{x}(0) = v$ and an initial displacement of $x(0) = 0$. The solution is a half-sine, with the duration of the impact being the second solution to $x(t) = 0$:

$$m\ddot{x} + kx = 0 \quad \Rightarrow \quad x(t) = \frac{v}{\omega_0} \sin(\omega_0 t), \quad \Rightarrow \quad t_{impact} = \frac{\pi}{\omega_0} = \pi \sqrt{\frac{m}{k}}, \quad (2.1)$$

where m is the mass, k the stiffness and ω_0 the natural frequency. The shortest impact is achieved with a small mass and high stiffness. The stiffness is limited by the violin bridge, which is made of maple wood.

Two B&K 8200 force transducers were available, one being part of a big impact hammer (B&K 8202). The big hammer was only used without a dedicated tip, while the standalone transducer was also used with three tips of varying stiffness. The equipment is shown in Figure 2.8.

The big hammer was held by the end of the handle and carefully swung against the bridge. The standalone transducer was held by its cable, and digitally manipulated to swing like a pendulum.

In order to mitigate the unreliability of the hammer method, each measurement consisted of 10 impacts, averaging the transfer functions for each impact. Each set of 10 measurements thus required 100 impacts.

The piezoelectric accelerometer was chosen for this investigation because the minimum sensitivity on the LDV was still prone to cause significant signal overload for some impact methods. While the accelerometer adds mass to the bridge, affecting both the force spectrum and the admittance, it should not alter how one impact method compares to another.

The measured bridge admittance for different impacts methods can be seen in Figure 2.9. The admittances are normalized to 250 Hz since two different transducers were used. Note how using the big hammer gives very bad results around 480 Hz, and how the soft tip diverges from the other



Figure 2.8: Force transducer, hammer and tips.

methods above 600 Hz. The results for no tip and the hard tip are generally in good agreement. (The medium stiffness tip gave results very close to the results with no tip and was omitted from the plots for better readability.)

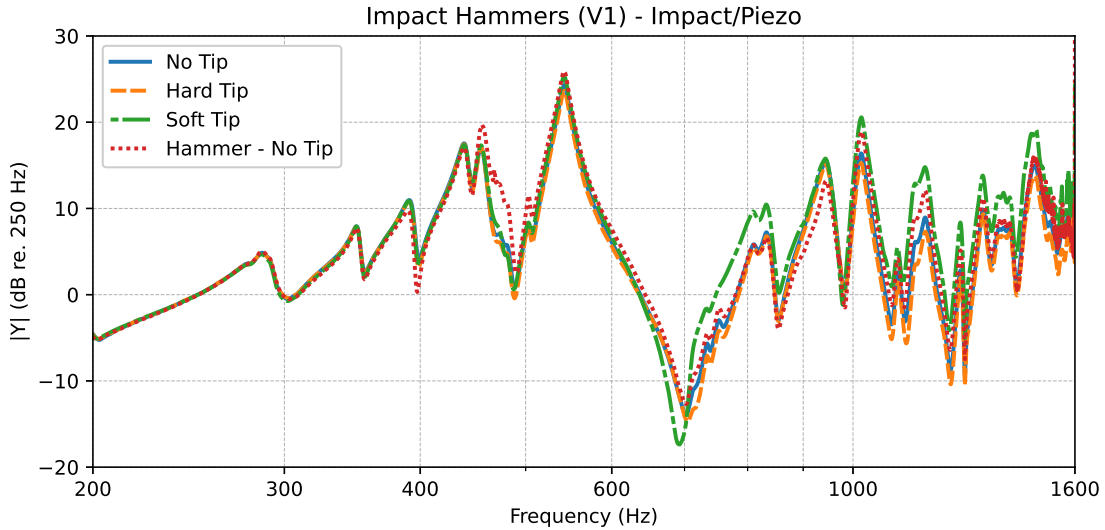


Figure 2.9: Bridge admittance for each impact method, normalized to 250 Hz.

The averaged time signals and amplitude spectra for the force are seen in Figure 2.10. Both have been normalized in order to highlight the differences in shape. The heavier and softer impacts have longer durations, the effect of which can be seen on the force spectrum. Notice how a large dip in spectral amplitude occurs around 480 Hz for the big hammer, where the admittance results were also bad.

The stand-alone force transducer was the lightest of all the different "impact hammers", with the shortest excitation signal and the flattest spectrum. For the rest of the thesis, this was used for all impact hammer measurements.

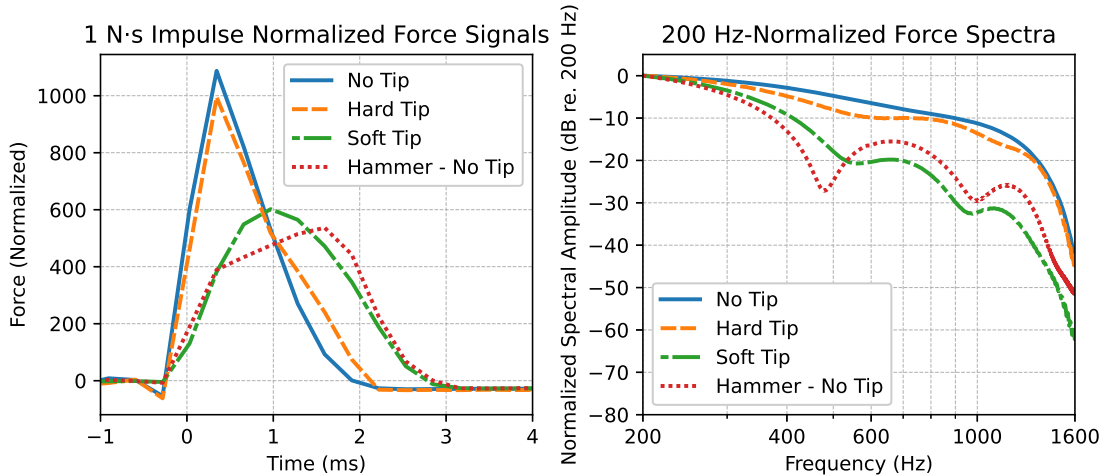


Figure 2.10: (Left) Time signals (force) for each impact method, normalized to a 1 N·s total impulse. (Right) Force spectra, normalized to the spectral amplitude at 200 Hz.

2.6 Violin support

There are two main benefits from ensuring free-free boundary conditions. One is that it allows direct comparisons to other instruments, and the other is that free-free boundary conditions are mostly unambiguous. However, it is not very practical, often places the instrument precariously and suffers from a lot of position-based uncertainty. Furthermore, the violin does not have free-free boundary conditions when played.

The holding method for this thesis is mostly identical to the previous projects [5, 6]. The violin was placed in a wooden frame, resting the lower bout on two shoulder-support feet, and the neck on a piece of rope. These points of contact are also present when playing the violin with a shoulder rest, and ensure a safe and reproducible placement of the violin. A drawing of the frame can be seen in Figure A.9 in the appendix.

The impact hammer method with the piezoelectric accelerometer was used because it was impractical to align the LDV for a variety of holding methods. Only a single 10-impact measurement was performed for each method since many were not set up to be reproducible. This should still be sufficient to reveal any major differences between measurements caused by the holding methods.

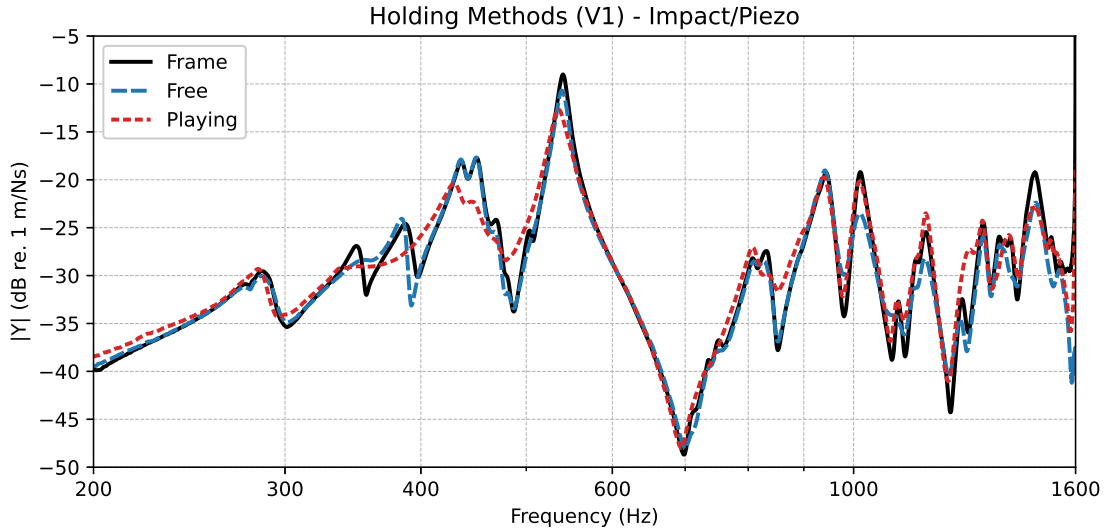


Figure 2.11: The bridge admittance for the frame, "free" boundary conditions and playing conditions (with shoulder rest).

Free boundary conditions were achieved by loosely suspending the violin by the screws, holding it with the thumb and index finger of the left hand, thus avoiding contact with the violin body. The bridge admittance was also measured when the violin was held for playing. These methods are compared to the frame in Figure 2.11. The frame and "free" support methods are a bit different in the 300-400 Hz region, where the frame support has an additional resonance at 350 Hz, but a less pronounced resonance at 390 Hz. Otherwise the two methods are very similar.

The admittance for playing conditions is very different from the two other methods, showing no resonances in the 300-400 Hz range, significant damping for the B1 resonances and a shift in the A0 resonance. Generally speaking, there is nothing to indicate that the frame support is a worse method than suspending the violin freely. The frame was therefore judged to be a serviceable holding method for violin measurements.

2.7 Sound Measurement

Sound radiation measurements are non-trivial. At the low frequencies, the microphone must be placed far away to avoid near-field effects (wavelength of 200 Hz is ≈ 1.7 m!), while interference between different parts of the violin begins to come into play at high frequencies. In order to obtain a somewhat accurate measure of the far-field radiation, it would thus require multiple microphone positions and an anechoic chamber for mitigating reflections [3], but this method does not align with the goal of this thesis.

Since the method is intended to work in most rooms, the microphone must be placed *very* close to the violin. Information about which frequencies actually reach the far-field is hereby lost in favor of obtaining a good SNR. In order to keep the method simple, only one microphone position should be used. It has been suggested that a single reading in front of the bridge is sufficient to capture the violin's behavior up to 800 Hz, which includes all the signature resonances [14]. Two microphone positions were considered to be particularly relevant:

- Placing the microphone right at the G-string corner of the bridge. This is where the velocity is obtained for the admittance measurement, making this position ideal for relating admittance and radiativity measurements.
- Placing the microphone where the violinist's ears would be, represented as a single position (centered about 10 cm above the end of frame). This could be particularly relevant for quality assessments.

The final radiativity measurement placed the microphone 5 mm from the G-string corner of the bridge, as can be seen in Figure 2.12.



Figure 2.12: Final radiativity method, with the microphone placed 5 mm from the bridge corner.

The two positions were tested by exciting the violin with a pendulum (see Chapter 4). The responses were normalized because the closer position resulted in a higher output level. The sound pressure responses (not radiativity) can be seen in Figure 2.13. Some acoustic egg-crate foam was placed beneath the frame to eliminate the strongest reflections, but it was found to be irrelevant for the pressure response at the bridge.

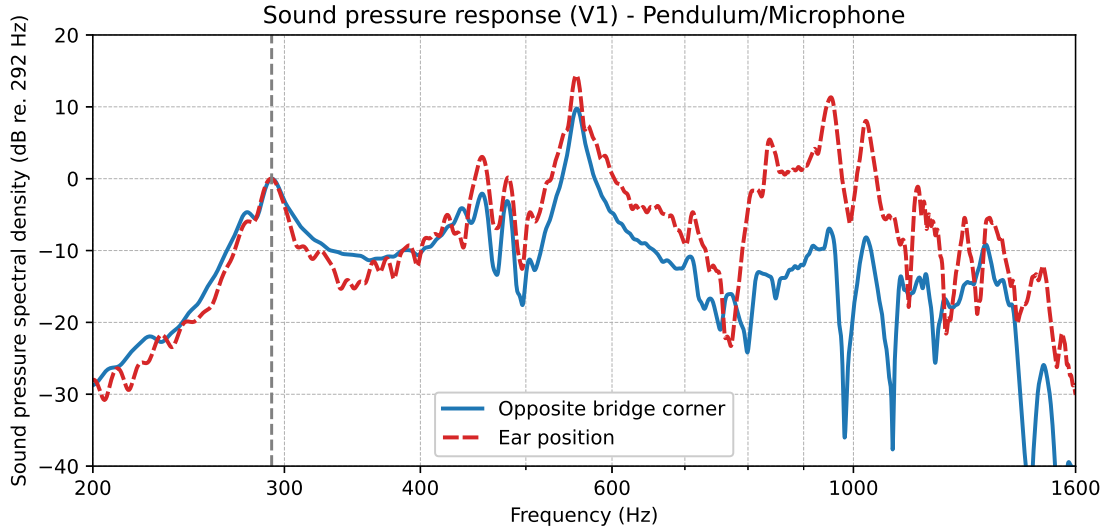


Figure 2.13: Sound pressure responses for two microphone positions.

The bridge response has a higher relative level at low frequencies which is attributed to the near-field effects. The ear position response is more noisy which is attributed to reflections. Both positions show very similar signature resonances, but the bridge position was chosen as superior due to a better signal-to-noise ratio and a less ambiguous microphone position.

2.8 Arduino Sensors

Two cheap sensors were tested in the pursuit of alternatives to the LDV and GRAS 46AE. These were the MEMS accelerometer ADXL345 [15] and the electret microphone MAX4466 [16]. These were controlled using an Arduino Nano V3. The wiring connections can be seen on Table 2.1, and pictures of the equipment in Figure A.2 in the appendix.

- **ADXL345:** Set up to use only the z-axis acceleration. Allows sampling rates up to 3200 Hz (was only used with 1600 Hz), with a 13-bit resolution and a ± 16 g range. Communication was set up to use the SPI communication protocol. Calibration was performed by measuring the ± 1 g signal output. Overload was sometimes a problem.
- **MAX4466:** Saved data to an SD-card using an SD-card module. The gain was adjusted to the minimum value, but overload was still a major problem.

Table 2.1: Arduino Nano V3 connections to the ADXL345, MAX4466 and SD-Card Reader.

*The SD card was powered by a separate power supply module.

Arduino Nano Pin	ADXL345	MAX4466	SD Card Reader
3.3V	VCC	VCC	-
5V*	-	-	VCC
GND	GND	GND	GND
A0	-	OUT	-
D2	INT1	-	-
D10	CS	-	CS
D11	MOSI (SDA)	-	MOSI
D12	MISO (SDO)	-	MISO
D13	SCK (SCL)	-	SCK

The ADXL345 was compared to the LDV by pointing the laser at a piece of reflective tape attached to the module. The MAX4466 was compared to the GRAS 46AE microphone at the ear position in order to avoid signal overload, which was detrimental to the results at the bridge position. The results can be seen in Figure 2.14, where the microphone gives usable results for the signature resonances, but does not measure the high frequencies accurately, likely due to a much higher noise floor. The accelerometer completely fails to replicate the LDV output, even when displaying only the best impacts. This investigation of cheap sensors was discontinued, but the MAX4466 did show some promise.

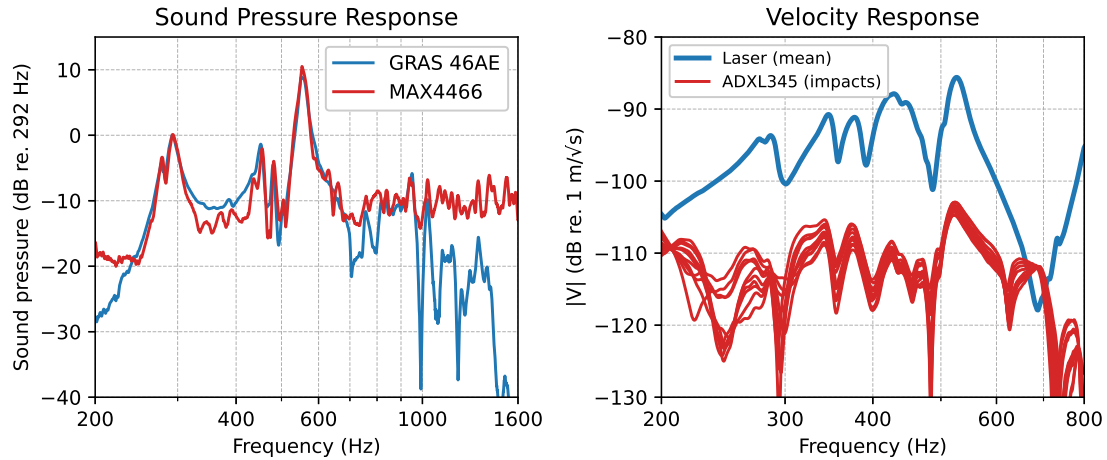


Figure 2.14: Results for ADXL345 and MAX4466 compared to the LDV and GRAS 46AE respectively.

Chapter 3 Mass Loading

Since the violin bridge has a mass of 2-3 grams it takes very little to change its mechanical properties. Therefore, any mounted transducer will usually cause a significant change in the measured admittance. This effect depends not only on the mass of the transducer, but also its position on the structure being investigated [17]. A practical way of evaluating this mass-loading effect is to compare the natural frequencies of the loaded and unloaded violin.

For very low frequencies, where the bridge is much smaller than the wavelength, the bridge can be assumed to act as a rigid body. Then the measured transfer admittance across the bridge will be identical to its input admittance, and the bridge and added mass from mounted transducers will have the same velocity. The force measured by the force transducer F_{meas} is simply distributed between the bridge and the added mass:

$$F_{meas} = F_b + F_m, \quad (3.1)$$

where F_b is the force applied to the bridge, and F_m is the force applied to the added mass. Rewriting $F_m = j\omega m V$ and converting to the frequency domain we get

$$\underline{Y}_b = \frac{\underline{V}}{\underline{F}_b} = \frac{\underline{V}}{\underline{F}_{meas} - j\omega m \underline{V}} = \frac{\underline{Y}_{meas}}{1 - j\omega m \underline{Y}_{meas}}, \quad (3.2)$$

where m is the added mass, \underline{Y}_b is the true bridge admittance and \underline{Y}_{meas} is the measured admittance. Note that the phase information is important, and that any delay between channels therefore must be accounted for. It was found that this correction does not work for eliminating the mass-loading of the shaker setup. For the piezoelectric accelerometer, the correction is very effective and it is possible to obtain very good results as seen in Figure 3.1.

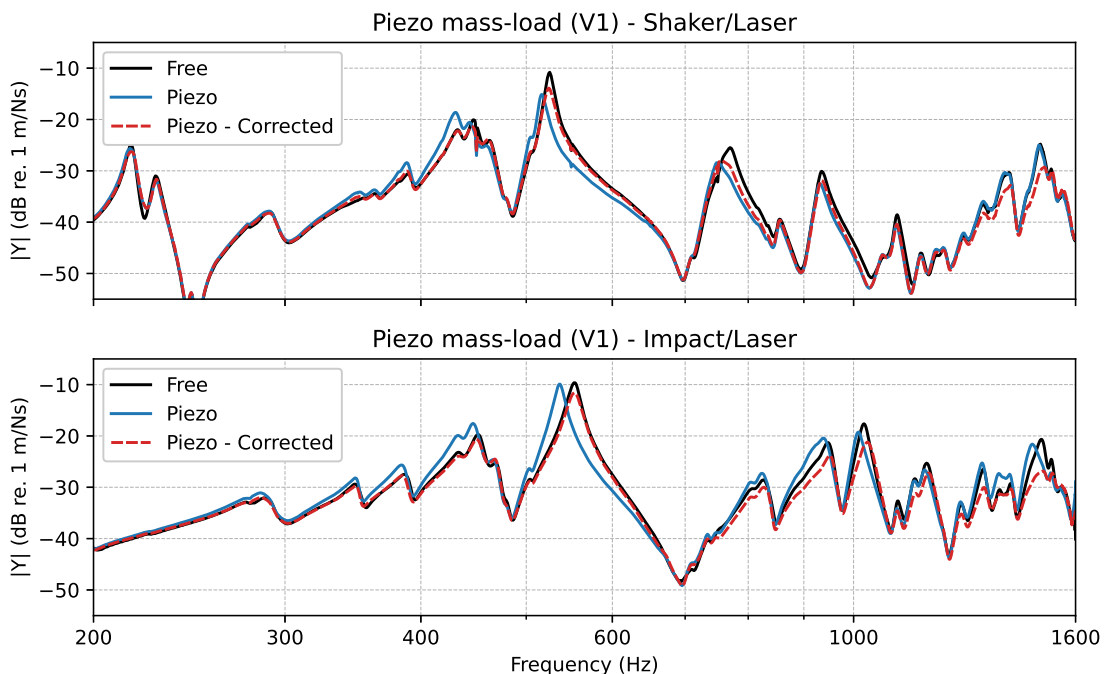


Figure 3.1: Mass-load correction for the piezoelectric accelerometer (effective mass ≈ 2.5 grams).

3.1 Mass-loading properties

One important question had to be answered in order to determine whether compensating for mass loading could be a viable method:

- Are mass loads the same for different violins?

Correcting for mass-loading effects is interesting because LDVs are very expensive. If an accelerometer has a known mass-loading effect, it potentially could work as a cheaper alternative with no downsides. This will not be possible if the effective mass loads are not the same for different violins. A less important, but interesting question was also investigated in order to better understand mass-loading:

- Is mass-loading linear?

It is assumed that for each violin and load there is an expected mass-loading effect. Measurements were conducted for two violins (V1 and V3), across six mass-loading configurations, one being the unloaded bridge. "ADXL" refers to the MEMS accelerometer from Section 2.8. Admittances for each mass load can be seen in Figure A.3 in the appendix.

- Free
- Piezo
- ADXL
- Mute
- Piezo & Mute
- ADXL & Mute



Figure 3.2: The violin bridge loaded with a mute (left), the piezoelectric accelerometer (middle) and the ADXL345 accelerometer (right).

The LDV was used with the impact hammer method, with three measurement sets conducted for each violin (V1a, V1b, V1c, V3a, V3b, V3c) for a total of 360 measurements consisting of 3600 impacts. The loads and violins were alternated to account for uncertainty from positioning the violins, LDV and loads.

The effective mass-load was determined by matching the B1+ resonance frequency of the loaded and free admittance. This resonance was chosen because it was prominent for both violins and very sensitive to mass loading. Due to the frequency resolution of 0.5 Hz, this match could be achieved with a range of mass values. The average of the smallest and largest valid masses was used for each case, with the guessed mass incrementing by steps of 0.01 grams. For each set, the free measurements were averaged to obtain a single reference B1+ resonance frequency and the effective mass load was calculated for each loaded measurement. This yielded 30 reasonably independent values per violin and load (two with 29 due to corrupted data). The combined distributions are shown in Figure 3.3.

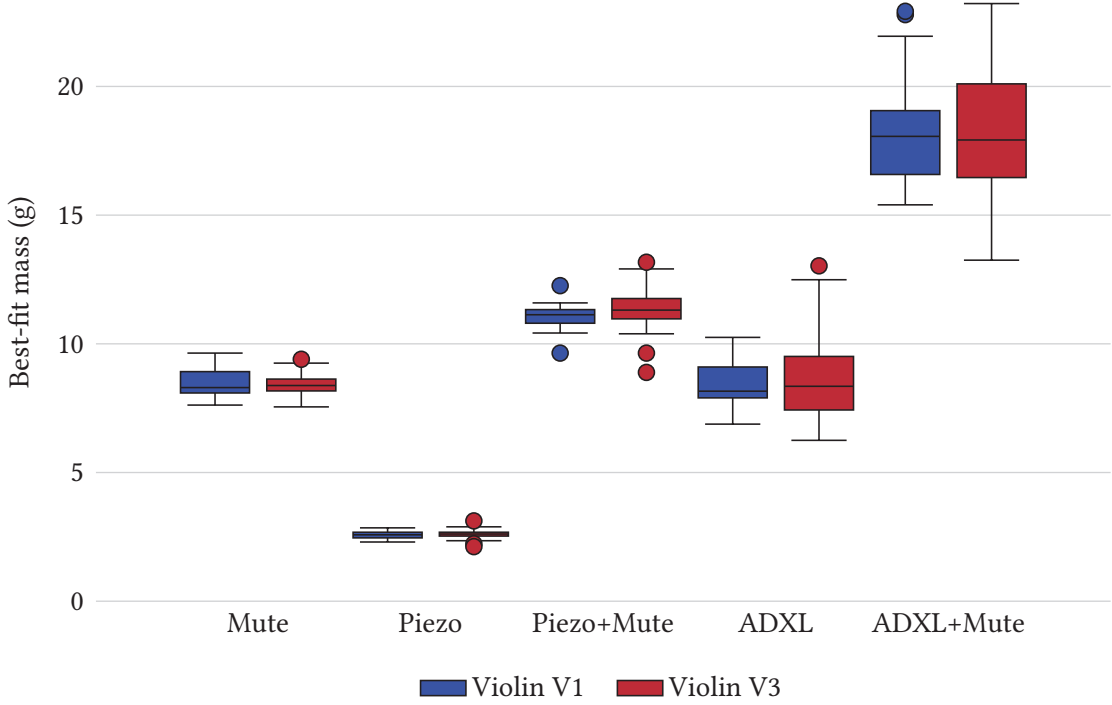


Figure 3.3: Boxplots for the effective masses of the different mass-loads. The boxplots for all sets can be seen in Figure A.4 in the appendix.

Notice that the spread for the mass estimates is greater for V3 in all cases except for the mute. The likely explanation is that the bridge for V3 was more narrow than for V1, meaning that attaching the two accelerometers with beeswax was more difficult.

Question 1 was tested with the null hypothesis that the mean of the effective-masses are the same for V1 and V3 for each load. Two-sample t-tests (Welch's) were performed with a significance level of $\alpha = 0.05$. Normality was assessed via QQ plots, showing sufficient linearity. Since the risk of false positives increases with the number of tests performed, the Bonferroni correction was used, adjusting the significance level $\alpha/5 = 0.01$ to account for the five tests.

Table 3.1: Best-fit mass values (g) for each load and violin.

Load	V1 Mean	\pm SD	V3 Mean	\pm SD	Mean Diff. (V1 - V3)	p-value
Mute	8.52	\pm 0.59	8.43	\pm 0.49	0.10	0.502
Piezo	2.58	\pm 0.15	2.61	\pm 0.20	-0.03	0.520
Piezo&Mute	11.08	\pm 0.47	11.33	\pm 0.89	-0.25	0.175
ADXL	8.42	\pm 0.89	8.74	\pm 1.82	-0.33	0.381
ADXL&Mute	18.29	\pm 2.16	18.14	\pm 2.51	0.15	0.810

The results can be seen in Table 3.1. The p-values are all much larger than 0.01, meaning that there is insufficient evidence to reject the null hypothesis that mass-loads are the same for the two violins. The effective mass-loads for V1 and V3 are thus statistically equivalent across all the tested loads.

Question 2 was tested with the null hypothesis that the mean masses of the combined loads Piezo&Mute and ADXL&Mute, are the same as the sum of the individual load means. One-sample t-tests were used, with the Bonferroni correction adjusting the significance level to $\alpha/4 = 0.0125$.

Table 3.2: Best-fit mass loads (g) for Piezo&Mute vs. summed means of individual loads.

Violin	Combined Mean	\pm SD	Sum of Means	Diff. (Comb. - Sum)	p-value
V1	11.08	\pm 0.47	11.10	-0.02	0.775
V2	11.33	\pm 0.89	11.04	0.29	0.081

Table 3.3: Best-fit mass loads (g) for ADXL&Mute vs. summed means of individual loads.

Violin	Combined Mean	\pm SD	Sum of Means	Diff. (Comb. - Sum)	p-value
V1	18.29	\pm 2.16	16.94	1.35	0.002
V2	18.14	\pm 2.51	17.17	0.97	0.043

Table 3.2 does not show significant differences, with the p-values > 0.0125 for both violins, meaning that the null hypotheses should not be rejected for the Piezo/Mute load. For these loads, the mass-load behaves linearly. This is not the case for the ADXL/Mute, as Table 3.2 shows that V1 deviates from linearity ($p = 0.002 < 0.0125$). While this could be a false positive, it does not matter, since mass loading of this scale is unnecessary and cannot be properly corrected for anyway.

3.2 Small Masses

Mass loading was also briefly investigated for some known masses. Two pieces of wood were cut and their masses estimated to about 0.15 g and 0.60 g.

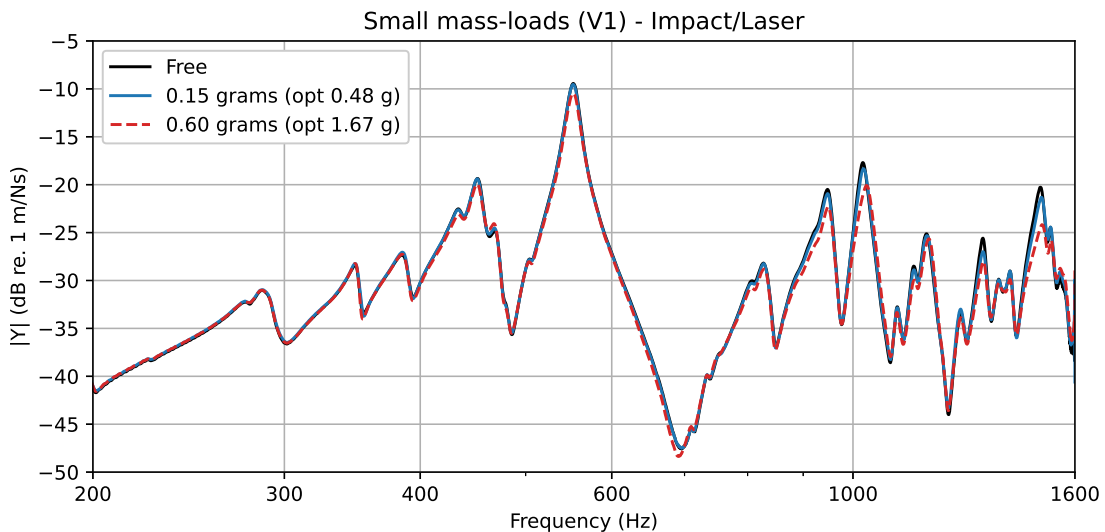


Figure 3.4: Mass-load correction for small pieces of wood.

The corrected FRFs for these loads can be seen in Figure 3.4, where it can be seen that the small mass allows near-perfect results for the entire 200-1600 Hz range. The larger mass shows greater deviation similar to the piezoelectric accelerometer. For a sensor of 0.15 g, mass-load correction could be a viable option with few drawbacks, especially if only the first few modes are desired. A heavier sensor is also viable, but suffers a bit at high frequencies. For the 1050 Hz mode, the small mass causes a shift of 2 Hz in resonance frequency and an amplitude drop of 0.5 dB, which is comparable to measurement uncertainty. Thus, a sufficiently small accelerometer could replace the LDV.

Chapter 4 Pendulum Excitation

An infinitely short impact has a perfectly flat spectrum, but even an impact lasting multiple samples will still be quite flat. Such a short signal can't contain much information, so the spectral information concerning the violin modes will be found almost exclusively in the response.

Different violins have different bridge admittances, so the input signals will also be different, even when using a perfectly reliable impact hammer. However, as the mass of the hammer decreases, so does the duration of the impact, see Eq. (2.1). The shorter the impact, the smoother the force spectrum will become and the less information it will contain. This is true for all violins, and in the limit, where the impact duration becomes smaller than a sample, there is no longer anything to distinguish between violins, except maybe a level difference. The spectrum will be perfectly flat in all cases.

In summary, if an excitation method supplies a sufficiently brief impact signal, then the force spectrum can be replaced by a constant weighting curve for all violins with very little uncertainty. It is proposed that this can be achieved with a simple pendulum. If the pendulum is configured to drop from a constant height, it should possess the same momentum every time it makes contact with the violin bridge, and thus require a constant impulse to be repelled.

A pendulum with near-zero mass is not practical so there will inevitably be some difference between the force spectra of different violins, which will add uncertainty to the method.

4.1 Pendulum Method

For a single violin, the procedure would be the following:

1. Perform a measurement of the "true" admittance using the impact hammer method.
2. Measure the pendulum response to obtain an estimate for the pendulum force spectrum.
3. Perform a new pendulum measurement and use the estimated force spectrum to obtain an estimate for the admittance.

The method is thus a simple 3-step calculation:

$$\underline{Y}_{true} = \frac{\underline{V}_{hammer}}{\underline{F}_{hammer}} \quad \rightarrow \quad \underline{F}_{est} = \frac{\underline{V}_{pend}}{\underline{Y}_{true}} \quad \rightarrow \quad \underline{Y}_{est} = \frac{\underline{U}_{pend}}{\underline{F}_{est}} \quad (4.1)$$

Here \underline{V}_{hammer} and \underline{F}_{hammer} refer to the velocity and force from the impact hammer method, \underline{V}_{pend} is the pendulum velocity response used to estimate pendulum force, and \underline{U}_{pend} is the pendulum velocity response used to estimate the admittance. The idea is for the estimated force spectrum \underline{F}_{est} to be computed for a representative sample of violins, after which only the 3rd step will be necessary.

4.1.1 Uncertainty

The 3-step procedure adds a lot of uncertainty compared to a single 2-channel measurement with an impact hammer, since the relative variances will compound at each step. The sample variances are computed empirically from the measurements.

Consider the estimated force \underline{F}_j for violin j , which is based on the measurements \underline{Y}_i using the impact hammer and \underline{V}_i using the pendulum. The magnitudes are used, discarding the phase

information to avoid unwanted cancellation. The estimated force spectrum \underline{F}_j is thus real-valued and positive, and is computed as

$$\underline{F}_j = \frac{|\bar{\underline{V}}|}{|\bar{\underline{Y}}|}, \quad \text{where} \quad |\bar{\underline{V}}| = \frac{1}{n_V} \sum_{i=1}^{n_V} |\underline{V}_i|, \quad |\bar{\underline{Y}}| = \frac{1}{n_Y} \sum_{i=1}^{n_Y} |\underline{Y}_i|, \quad (4.2)$$

where n_V and n_Y are the number of measurements for each method, and $|\bar{\underline{V}}|$ and $|\bar{\underline{Y}}|$ are the sample means of $|\underline{V}_i|$ and $|\underline{Y}_i|$. For this thesis $n_V = n_Y = 10$. If the number of violins is N , then the sample mean of the estimated force (averaged across violins) will be

$$E[\underline{F}_j] = \bar{\underline{F}} = \frac{\sum_{j=1}^N \underline{F}_j}{N}. \quad (4.3)$$

It is assumed that each of the estimates \underline{F}_j is normally distributed around its expected value μ_j , and that these group means across N violins follow a normal distribution centered on the overall mean $\bar{\mu}$. Assuming normal distributions is not strictly necessary for the calculations, but allows for easier interpretation of deviations. Since the hammer and pendulum measurements are independent, the relative variances compound in the following manner

$$\frac{\text{Var}(\underline{F}_j|\mu_j)}{|\underline{F}_j|^2} = \frac{\text{Var}(|\bar{\underline{V}}|)}{|\bar{\underline{V}}|^2} + \frac{\text{Var}(|\bar{\underline{Y}}|)}{|\bar{\underline{Y}}|^2} = \left(\frac{s_V^2}{n_V |\bar{\underline{V}}|^2} + \frac{s_Y^2}{n_Y |\bar{\underline{Y}}|^2} \right), \quad (4.4)$$

where s_V^2 and s_Y^2 are the sample variances of $|\underline{V}_i|$ and $|\underline{Y}_i|$. This is the uncertainty for the estimate \underline{F}_j for a specific violin, around its expected value μ_j . The law of total variance is used to account for the differences between violins,

$$\begin{aligned} \text{Var}(\underline{F}_j) &= E[\text{Var}(\underline{F}_j|\mu_j)] + \text{Var}(E[\underline{F}_j|\mu_j]) \\ &= \frac{\sum_{j=1}^N \text{Var}(\underline{F}_j|\mu_j)}{N} + \frac{\sum_{j=1}^N (\underline{F}_j - \bar{\underline{F}})^2}{N-1}. \end{aligned} \quad (4.5)$$

This is the variance of the estimate \underline{F}_j for *any* violin, and represents the uncertainty when applying the estimated pendulum force spectrum to an unknown violin. Applying the method is simple, once the estimated force spectrum and its uncertainty have been computed. A new set of pendulum velocity responses U_i are introduced for the third step of the procedure,

$$\underline{Y}_{est} = \frac{|\bar{\underline{U}}|}{\bar{\underline{F}}}, \quad |\bar{\underline{U}}| = \frac{1}{n_U} \sum_{i=1}^{n_U} |\underline{U}_i|, \quad (4.6)$$

where $n_U = 10$ is the number of measurements and $|\bar{\underline{U}}|$ is the sample mean. The relative variance is then,

$$\frac{\text{Var}(\underline{Y}_{est})}{|\underline{Y}_{est}|^2} = \frac{\text{Var}(|\bar{\underline{U}}|)}{|\bar{\underline{U}}|^2} + \frac{\text{Var}(\bar{\underline{F}})}{|\bar{\underline{F}}|^2} \quad (4.7)$$

This method is tested in the following sections.

4.1.2 Smoothing

It is necessary to apply smoothing to \underline{F}_{est} in order to obtain a more realistic estimate. A 1st order Savitzky–Golay filter with size 301 is applied twice to the estimated force spectrum. This smoothing procedure was determined by experimenting with different methods in an attempt to get something that looked reasonable.

4.2 Proof of concept

The cord-held force transducer was used for the proof of concept since it has a known flat spectrum (see Section 2.5). With practice, the handheld impacts became very consistent, allowing it to serve as a concept pendulum, albeit with more variability in level. Example measurements for both violin V1 and V3 can be seen in Figure A.5 in the appendix. The entire procedure described in Eq. 4.1 was followed for both violin V1 and V3 using the piezoelectric accelerometer.

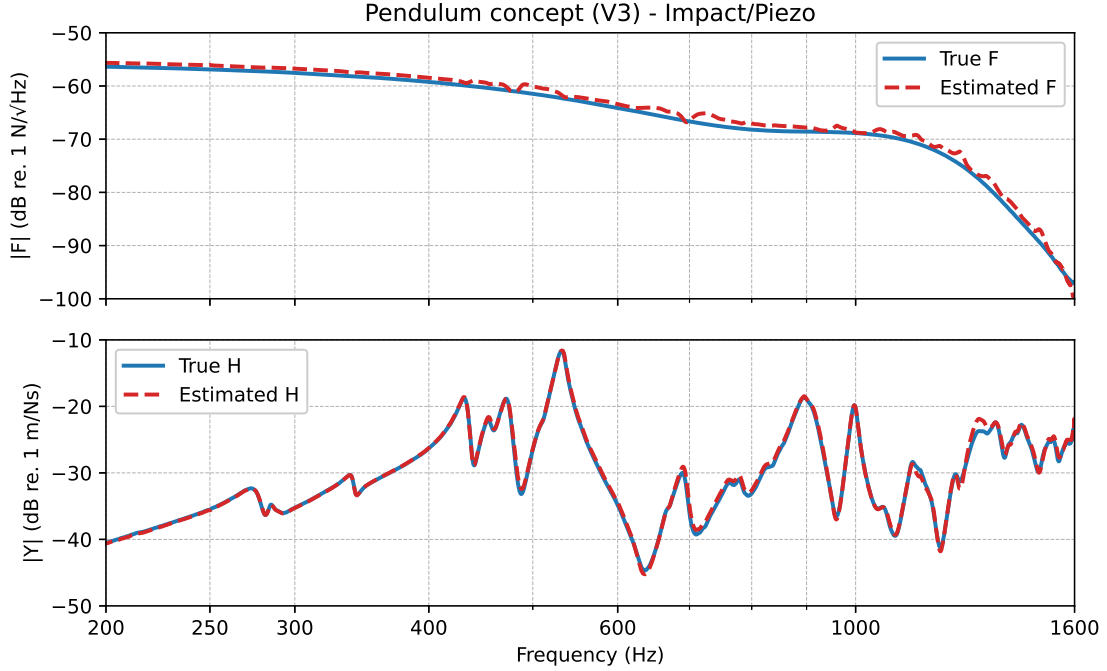


Figure 4.1: Estimated and true force and admittance.

The results of the concept test on violin V3 can be seen in Figure 4.1. There is a small level difference between the true and estimated force and admittance spectra, but this can be explained by the variability of the handheld impact. This variability coincidentally evens out the difference for the estimate of the admittance. Note that the estimated force spectrum is not completely smooth. These peaks and dips cannot reflect the actual force spectrum, which must be smooth due to its short duration. It is not a big problem in this case, but this roughness becomes a much larger problem for different pendulums. While the handheld impact hammer is very consistent, it is not a viable method for reproducibility in the long term. It has served as a successful proof of concept.

4.3 Designing the Pendulum

The requirement for the pendulum is a consistent impact with a short duration to minimize differences between violins. Multiple pendulums were tested with varying masses. Five pendulums with varying masses were tested and compared to the cord-held transducer:

- Transducer
- Heavy
- Medium
- Light - long
- Light - medium
- Light - short

Images of the different pendulums can be seen in Figure A.6 in the appendix. The piezoelectric accelerometer was used to avoid signal overload for the heavy pendulum.

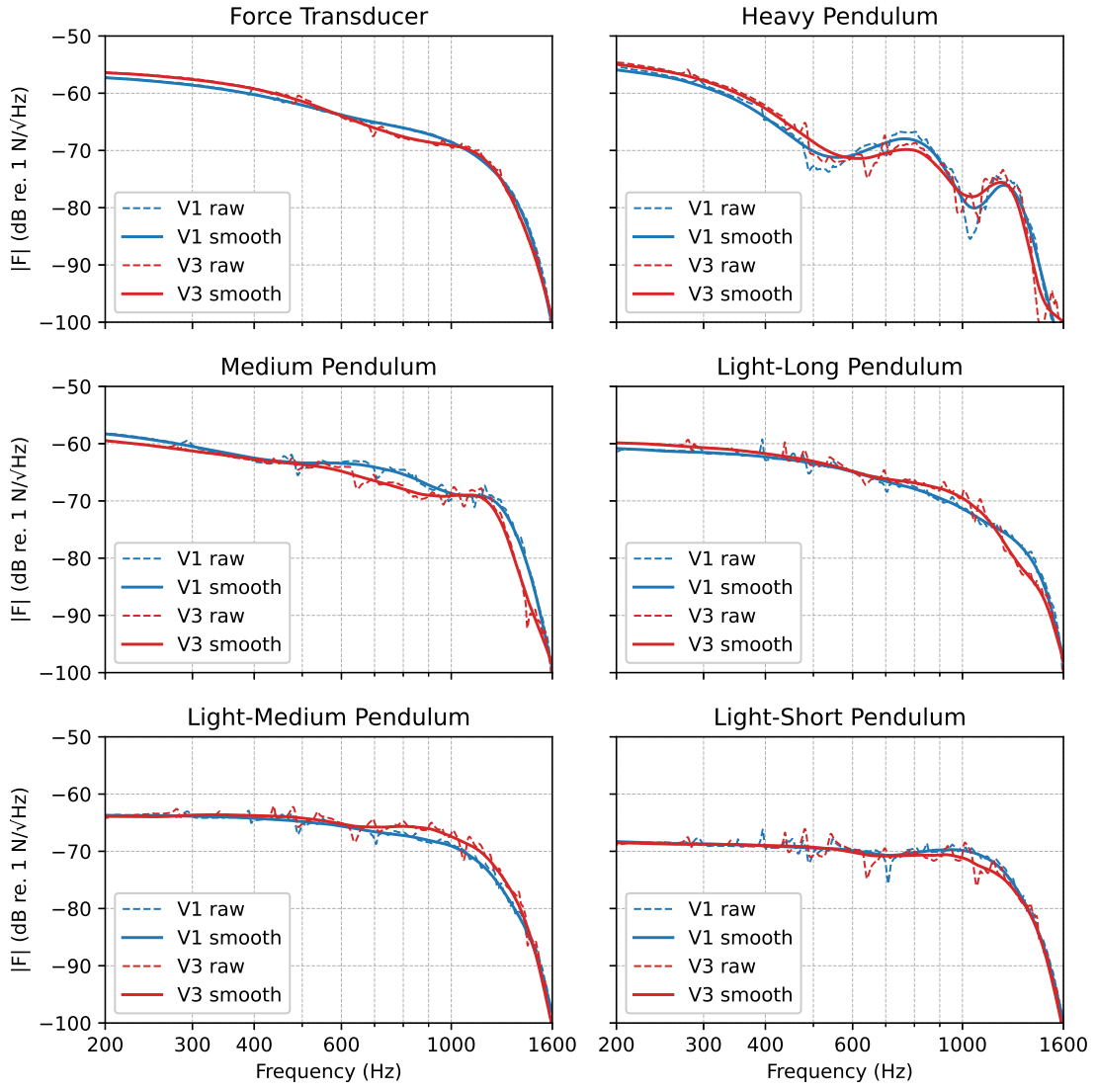


Figure 4.2: Force spectrum estimates for each pendulum for violins V1 and V3.

Figure 4.2 shows the estimated force spectra for all the pendulums for violins V1 and V3. Notice that the roughness of the spectra is much greater for the pendulums than for the transducer. The reason for this is likely that the violin responds differently to the various types of impact excitation, so the "true" admittance actually depends on the pendulum. It is not known whether these differences are due to the impact surfaces, pendulum masses or something else. A smoothing filter was applied to eliminate this roughness, giving a more realistic estimate. This also makes it easier to see the differences between the pendulums.

The light-short pendulum was chosen as the best candidate, showing minimal differences between the two violins up to 600 Hz. An even lighter pendulum was also tested, but its impacts were not consistent.

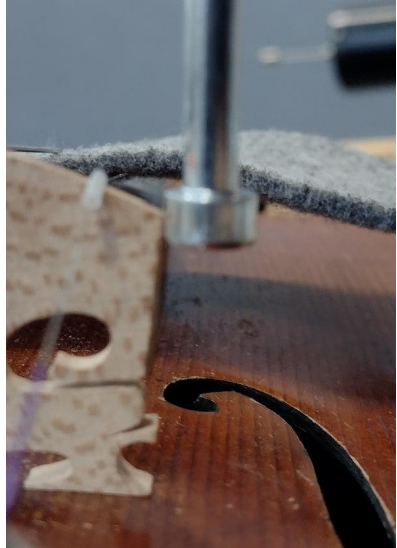


Figure 4.3: Pendulum position.

4.4 Final Pendulum

To ensure that impacts are as similar as possible, the pendulum and violin bridge should be aligned such that the edge of the pendulum tip is almost parallel with the edge of the bridge, see Figure 4.3. The point of contact should still be the corner of the bridge. Since the pendulum fixture was used with only two degrees of freedom, one rotational and one translational, this meant that the axis was in approximately the same position each time.

The entire pendulum setup can be seen in Figure 4.4, with a drawing in Figure A.10 in the appendix.

The LDV was used for the final method. The force spectrum of the pendulum was estimated from three violins V1, V2 and V3. The estimates were averaged and smoothed to obtain the final estimate F_{est} . The total relative variance was estimated as the combination of the relative inter- and intra-violin variances as per Equation (4.5). The pendulum fixture was reset between each measurement.

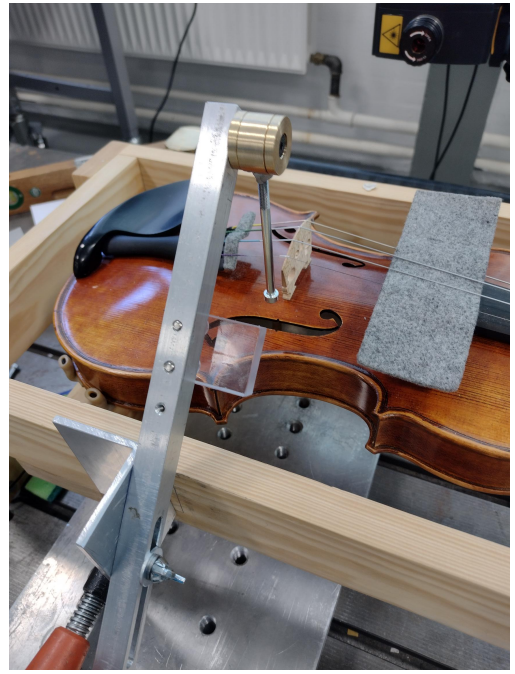


Figure 4.4: Pendulum setup with laser in the background.

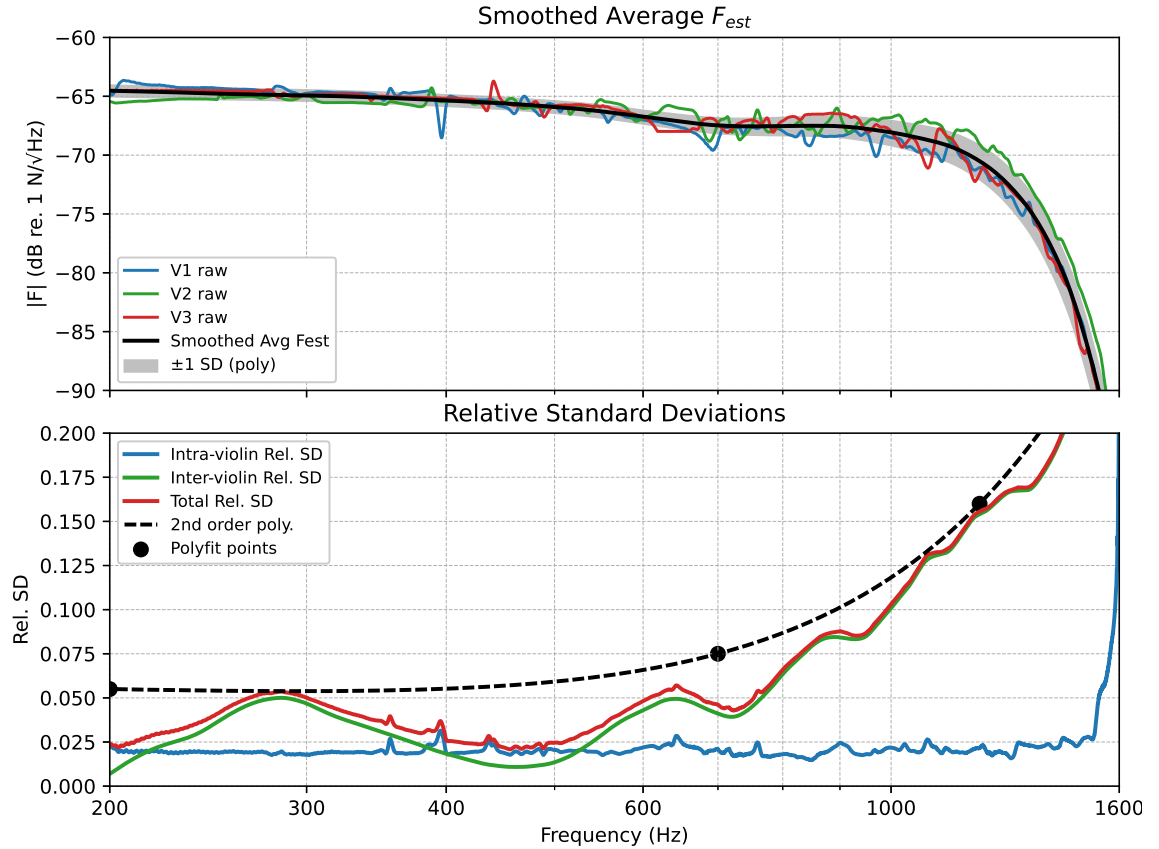


Figure 4.5: Estimated force spectrum for the final pendulum, as well as the relative standard deviation of the estimate. The inter-violin variance is based on smoothed force estimates for each violin. The shaded area for the estimate is based on the polynomial fit of the relative standard deviation.

The results for the smoothed average of the raw estimates and the inter-violin variability of smoothed estimates are shown in Figure 4.5. In order to get a better estimate of the inter-violin variability of all violins, it was assumed that the relative standard deviation would always increase with frequency. A simple 2nd order polynomial was fitted to some manually selected points to generate an envelope for the relative standard deviation. This is believed to be a better estimate of total variance for F_{est} . This also fits well with the inter-violin variability of the raw estimates, as seen in Figure A.8 in the appendix.

It is important to note that the deviation per frequency bin is not independent of the neighboring bins. Since the true force spectrum must be smooth and relatively flat, a deviation of +0.5 dB at 300 Hz, means that the deviation at 301 Hz will also be very close to +0.5 dB. This is important, since it means that the uncertainty of F_{est} does not significantly influence the frequencies and Q-factors of the resonances. It is thus the level of frequency bands that is most affected by the uncertainty of the estimate.

The inter-violin uncertainty is much larger than the intra-violin uncertainty. This means, that when applying the method to new violins, it will still be the uncertainty of F_{est} which dominates. We thus have a good estimate of the uncertainty of any measurement performed with the pendulum method. For the 200-700 Hz range it means that the final results will have an uncertainty of about ± 0.6 dB. Put into context, it has been found that when presenting single notes, the JND for the modes of the violin was 3-5 dB for amplitude and 3-5 % for the frequency of the modes, while the JND for frequency bands was closer to 1-3 dB and 1-3 % [18]. The uncertainty of the method is therefore so small that it should not pose significant problems for the accuracy of quality investigations.

The results from applying the method to violin V3 can be seen in Figure 4.6. The "true" admittance found with the impact hammer method mostly lies within a standard deviation of the mean admittance for the pendulum method. The discrepancies are largest at the anti-resonances, which is not a problem.

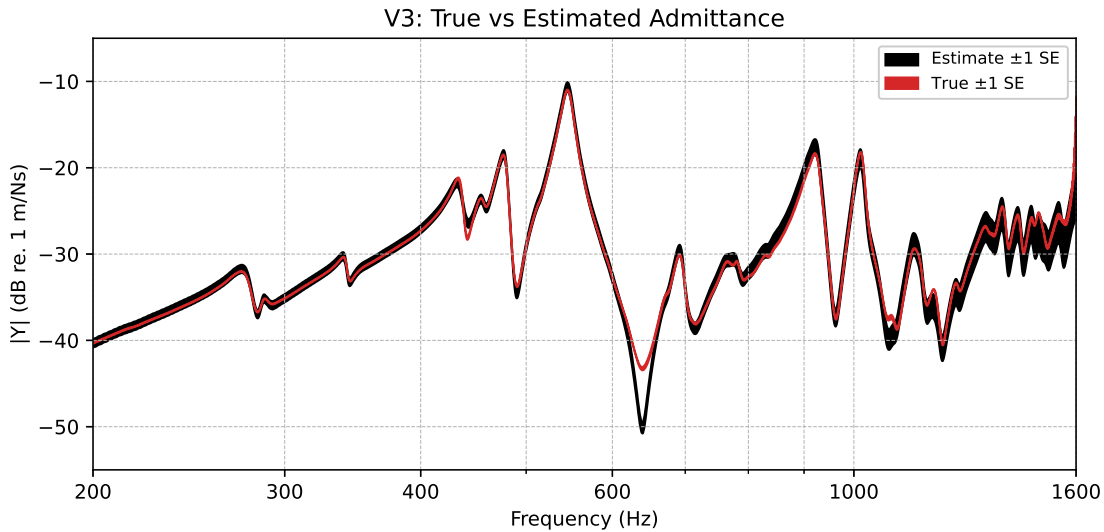


Figure 4.6: Bridge admittance from impact hammer method compared to the pendulum method.

Chapter 5 Pendulum Results

5.1 Measurement Setup and Playing Test

A total of 8 violins were measured using the pendulum method, acquiring bridge admittance using the LDV and radiativity using the GRAS 46AE microphone. The standard procedure of calibrating the equipment, tuning the instruments and damping the strings was followed.

Playing tests were conducted by two volunteers (inexperienced with quality assessments) who provided a single grading for each of the following quality descriptors:

- Overall rating
- Projection
- Balance
- Tone

These correspond well with the three dimensions for the semantic mapping of overall quality found by Fritz et al. [4]:

- Loud-Weak (projection)
- Uneven-Soft (balance)
- Rough-Clear (tone)

All measurements and playing tests were conducted within a few hours on June 19th, 2025.

5.2 Quality Assessment Results

The original results can be seen in Table B.1 in the appendix. The grading for *overall rating* was converted to a 1-3 scale, with 3 being the best. The grading for *projection* and *balance* was converted to a binary 1-2 scale, with 2 reflecting large projection and good balance respectively.

Tone was described with the words: "Grainy", "Sharp", "Dark", "Raspy", "Pure" and "Bright". These were interpreted as either "Clear", "Dark", "Sharp", or "Rough" in accordance with [4].

Table 5.1: Quality assessment for the 8 violins.

Violin	V1	V2	V3	V4	V5	V6	V7	V8
Rating	2	1	1	2	3	3	2	1
Projection	1	1	2	2	2	2	2	1
Tone	Rough	Rough	Sharp	Dark	Clear	Clear	Clear	Rough
Balance	2	1	2	2	2	2	1	1

The results can be seen in Table 5.1. For the *tone* of the violins, only "Rough" and "Clear" were used for multiple violins. Violins V3 and V4 were therefore ignored for this quality parameter. Note that the "Rough" tone perfectly coincides with a lower projection.

The players commented that it was immediately obvious to them which violins they preferred.

5.3 Measurement Results

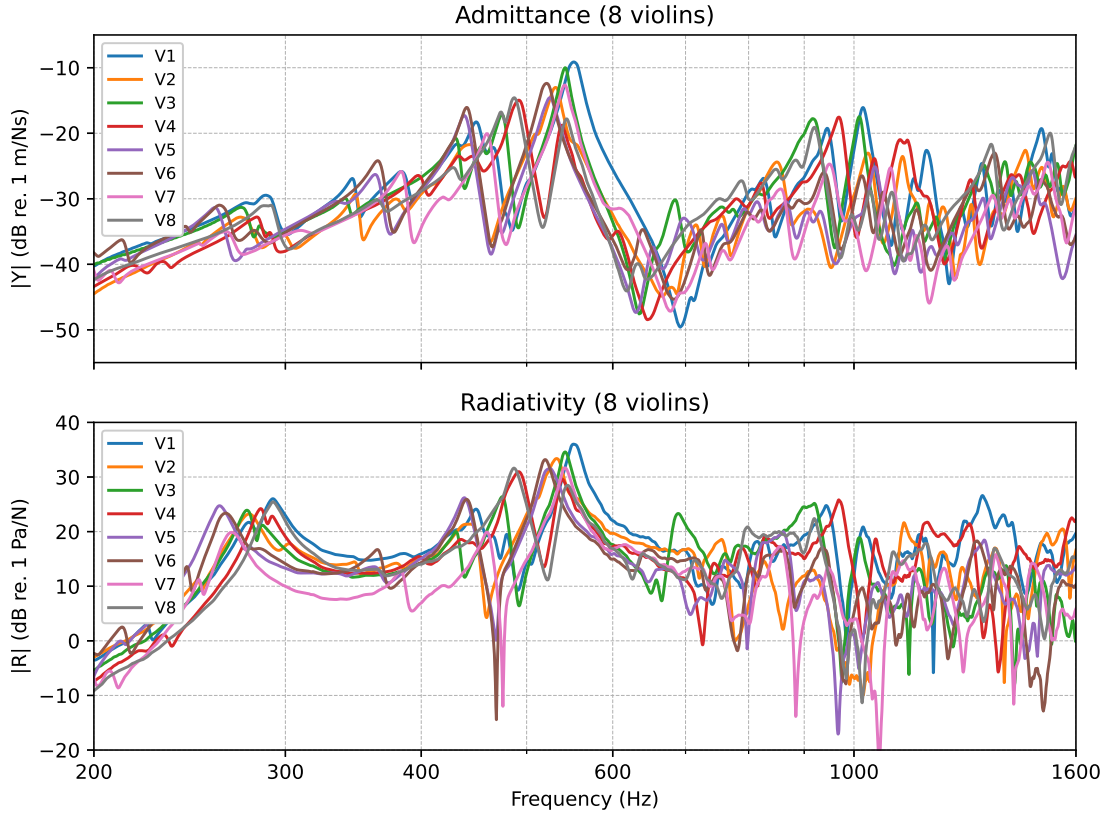


Figure 5.1: Admittance and radiativity results with the pendulum method for all 8 violins.

The admittance and radiativity results are seen in Figure 5.1. Only the signature resonances A0, CBR, B1- and B1+ were considered, since they were easily identifiable in most of the FRFs. For each of these resonances, the frequency, level and Q-factor were determined. The results for each violin can be seen in Figures B.1-B.4 in the appendix. The CBR resonance was often quite weak, especially for radiativity. It was only included if its peak value was at least 3 dB above the nearby FRF, making estimating the Q-factor possible. The Q-factor was difficult to determine for the A0 resonance due to some violins displaying another resonance at a similar frequency. This was judged to be the B0 "neck mode", which has previously been linked to improved sound quality when close to the A0 mode [19], and could thus be worth investigating in the future.

Since the admittance and radiativity are related, it makes sense to investigate how the signature resonances for the two FRFs compare. On Figure 5.2, the relationship between admittance and radiativity is seen for the frequency, level and Q-factor of the signature resonances, with a best-fit linear regression for each of them. For frequency, there is almost perfect correlation for all the signature modes with a fixed slope of 1. The CBR, B1- and B1+ resonances have the same frequency for both responses, while the A0 resonance was consistently 3 Hz higher in frequency for the radiativity compared to the admittance. It can thus be concluded that the admittance and radiativity measurements contain the same information with regards to signature resonance frequencies.

For the peak level, the correlation is weaker. Note that the slopes of the best linear fit vary a lot for the different modes, indicating a nonlinear relationship between the levels of admittance and radiativity. With R^2 values close to 1 it is once again indicated that the admittance and radiativity contain mostly the same information concerning the levels of the resonances.

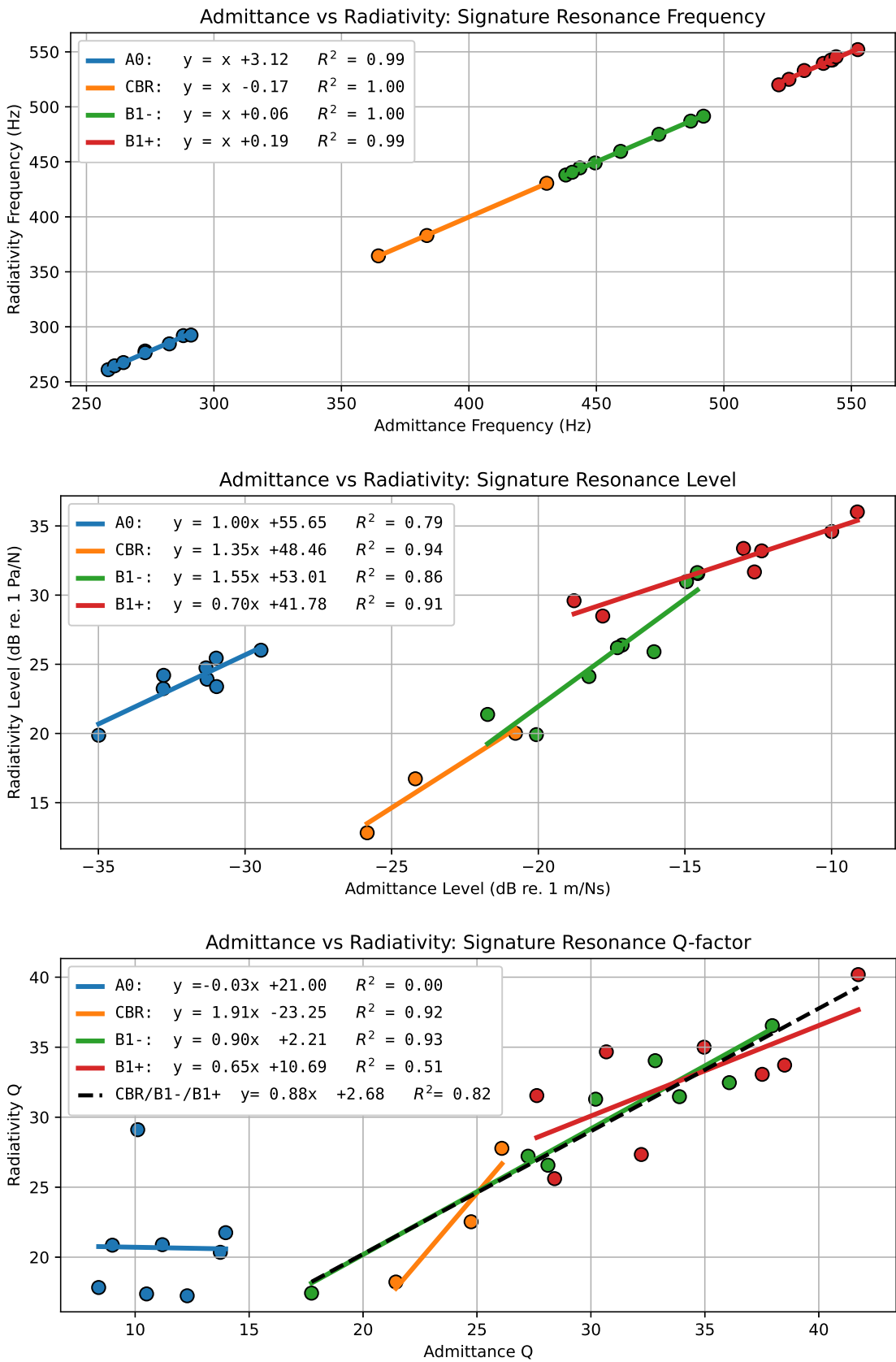


Figure 5.2: Comparison of signature resonance parameters for admittance and radiativity.

The Q-factors show good correlation for the CBR and B1- modes, while there is weak or no correlation for the A0 and B1+ modes. When collecting the three high frequency signature modes, a strong correlation of 0.82 emerges for the entire group.

Generally speaking, it appears possible for the radiativity to serve as a stand-in for the admittance measurement for the purpose of investigating the signature resonances, with only the A0 Q-factor showing bad correlation. More violins would need to be measured for more robust conclusions to be drawn.

5.4 Admittance/Radiativity transfer function

The correlation between admittance and radiativity led to the idea that there might exist a simple transfer function between the two. Specifying the admittance as \underline{Y} and radiativity as \underline{R} , the transfer function $\underline{H} = \underline{R}/\underline{Y}$ will have the physical unit Pa/(m/s). This directly relates the vibrational velocity of the bridge to the measured sound pressure next to the bridge. The transfer function for each violin can be seen in Figure 5.3.

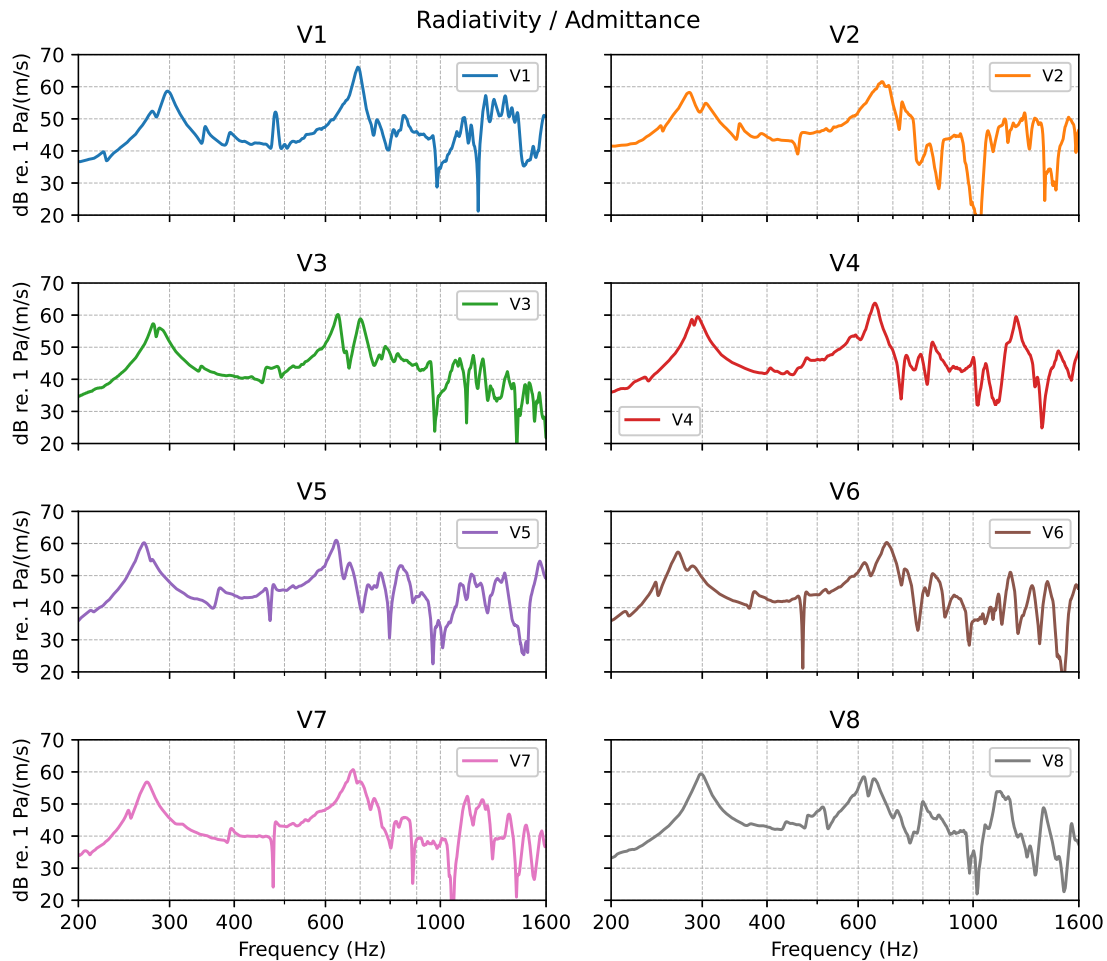


Figure 5.3: Radiativity/Admittance transfer function for each violin.

For all violins, there is a big peak at the A0 resonance. This is followed by a wide and relatively smooth valley that ends with a peak around 600-700 Hz. This range includes the signature resonances for all violins and is therefore worth taking a closer look at. After the second peak, the similarity between violins ends.

For each violin, the frequency axis is shifted to align the A0 resonance frequency (for radiativity) to 0 Hz. A running average of size 7 was used, gradually increasing to size 51 between 30 and 40 Hz. The shifted transfer functions are shown in Figure 5.4 along with the running average. There are significant differences in the level of the transfer functions, with differences between the largest and smallest value increasing to 10 dB at 350 Hz above the A0 resonances. This supports the findings of a nonlinear relationship between the magnitudes of the signature resonances for admittance and radiativity. The fact that the transfer function is quite flat for the CBR, B1- and B1+ resonances tracks with the correlation of their Q-factors.

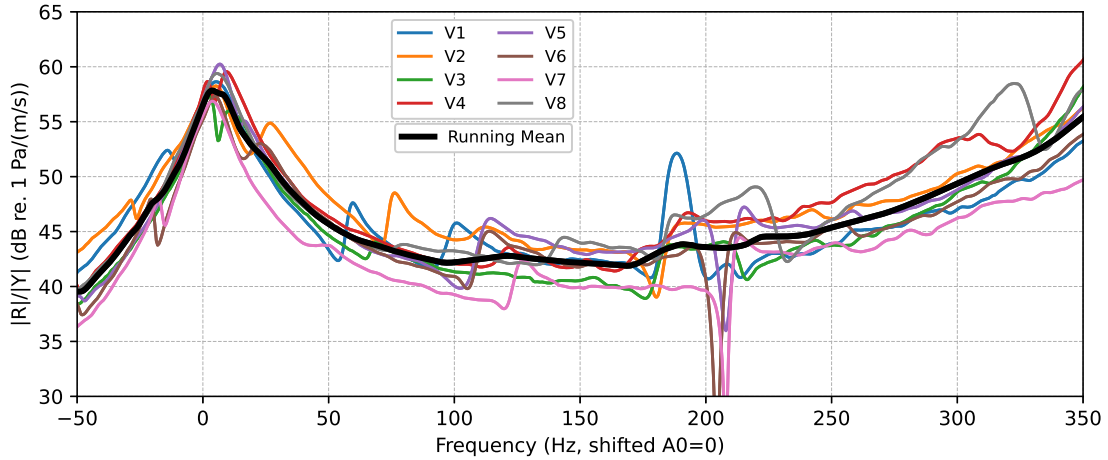


Figure 5.4: Shifted transfer functions for all violins with the running average in black.

The averaged transfer function was applied to the radiativity results as a weighting curve aligned with the A0 resonance. As can be seen in Figure 5.5, the effectiveness of this approach varies a lot. The B1- and B1+ estimates are pretty accurate, supporting the idea that the radiativity measurement can replace the admittance measurement. The A0 and CBR estimates are less reliable, but the method clearly replicates the admittance curve in general terms.

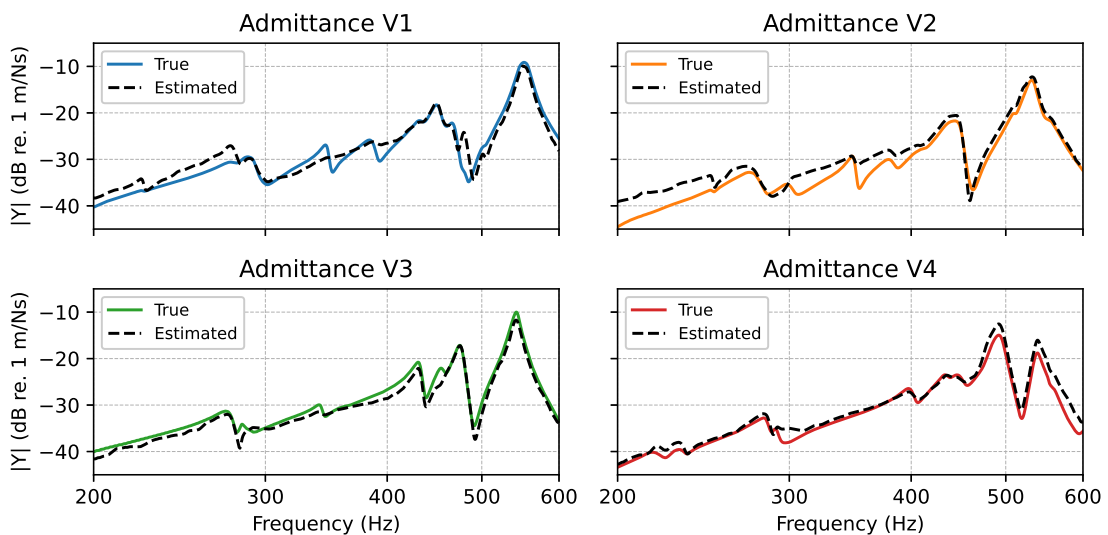


Figure 5.5: Averaged radiativity/admittance transfer function applied to the radiativity results.

5.5 Quality Link

With a sample size of 8 violins, and a low-resolution quality rating, it is not possible to find any meaningful correlation between measurements and quality. Either the quality rating would need better resolution, making it possible to perform a meaningful linear regression, or the sample size would have to be much larger, allowing for statistical tests. Therefore this investigation should be considered a pilot study, testing how to use the measured responses to find quality links.

The quality ratings were related to a number of signature resonance parameters extracted from the measurements: Frequency, relative frequency, level, relative level and Q-factor. This was done for both admittance and radiativity, but no link to quality was found. The results for frequency are seen in Figure 5.6, while the rest of the results have been omitted from the thesis.

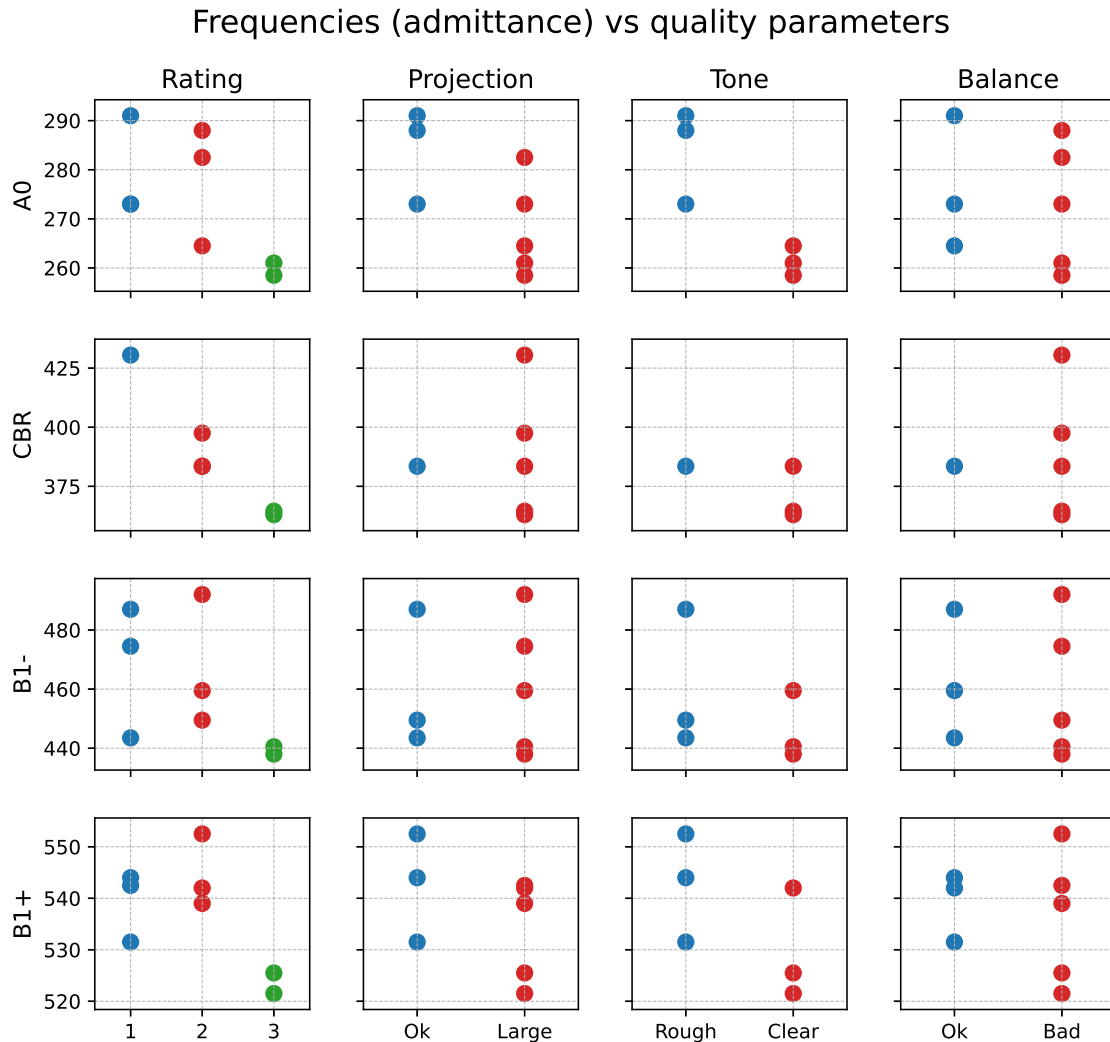


Figure 5.6: Quality ratings related to the signature resonance frequencies of the admittance measurement.

Of all the numerous comparisons (including the ones not shown), the only one with multiple samples in each quality category and no overlap between categories, is the relationship between A0 frequency and *Tone*. With only six samples, this is not significant, and it is rather surprising that only one of such cases was found.

Perhaps a more meaningful link between quality and measurements can be found by visual inspection of the results. It turns out that violins 4 and 8 are very similar, and that violins 5 and 6 are extremely similar. The admittance and radiativity results can be seen in Figure 5.7.

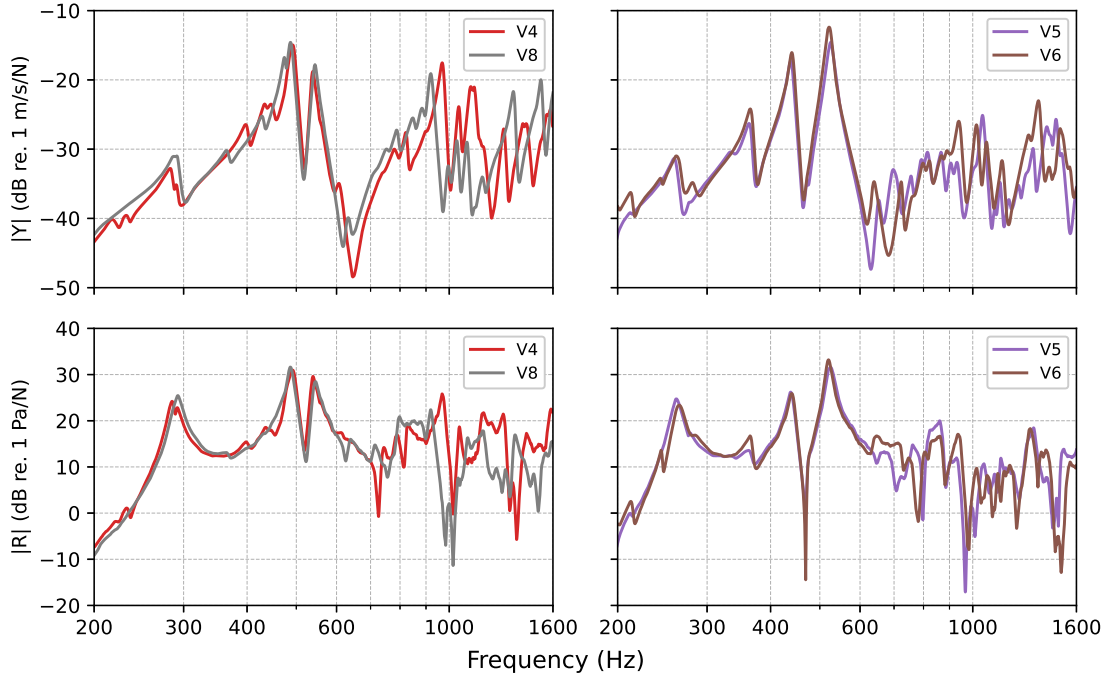


Figure 5.7: Results for violins V4 and V8, and violins V5 and V6.

V5 and V6 are almost identical and were given the exact same quality ratings as can be seen in Table 5.1. V4 and V8 are mostly the same for both FRFs, with the biggest difference being above 700 Hz, and they scored differently for every single descriptor. Assuming that the quality ratings are trustworthy (they aren't), this would indicate that the quality is not determined solely by the signature resonances, and that the high frequency content must be accounted for in some way.

The two violins with the best overall rating are V5 and V6. As can be seen on Figure 5.6, these have the lowest frequency signature resonances, which is the exact opposite of earlier findings [2]. A new investigation with more violins is warranted, most importantly with a more robust quality assessment.

Chapter 6 Discussion

Measurement Methods

The choice of string damping method was found to be quite important. It turns out that much of the literature on violin acoustics has been using string damping methods that are far from ideal. Hopefully the findings of this thesis will be considered, and a standard for string damping established.

While the simple mass-loading correction showed promise, perhaps a better correction scheme can be designed. Using this will unfortunately complicate the pendulum method, also requiring an estimate for the phase of the impact spectrum.

The pendulum was demonstrated to be a viable replacement to an impact hammer, decreasing the cost of the measurement method. Given that the inter-violin variance is the main source of uncertainty, an improved pendulum would be the most obvious point of improvement for the measurement method. With an even shorter impact, the measurement reliability should improve significantly. It should also be possible to extend the frequency range of the method to include the bridge hill. A specialized fixture for increased reliability and ease of use would also be a significant improvement.

The radiativity and admittance for the bridge appears to contain mostly the same information concerning the signature resonances. In combination with the pendulum method, this means that the only costly equipment necessary for investigating the signature resonances will be a microphone and DAQ device. This is a huge decrease in cost compared to the initial method. It appears that the radiativity measurement is an easier and better method of obtaining quantitative data on violins, while being more obviously relevant to perceived quality. For the relationship between admittance and radiativity, only the simplest transfer function was constructed. A more accurate transfer function could potentially be designed, taking the levels of signature levels into account in order to account for issues relating to nonlinearity. It might also be possible to extend the transfer function to give reasonable estimates for the higher frequencies, strengthening the idea that the radiativity measurement is sufficient.

The simplicity and affordability of the pendulum and radiativity measurement is of great benefit for making violin measurements accessible to more researchers. Making standardized violin measurement equipment widespread would make it possible to collect a large amount of comparable data that would enable large-scale quality investigations.

Quality Assessment

The biggest challenge for the attempt to link measurements to perceived quality was the accuracy of the quality assessment, and to a lesser extent the violin sample size. The participants were not familiar with performing quality investigations, so it does not make sense to use the findings for finding links to the signature resonances. A more reasonable conclusion to draw from the playing test is that even players unfamiliar with quality assessment can clearly perceive differences in violin quality.

The room acoustics for the quality assessment were quite bad, and only one set of grades was provided for each violin. Since the players were also the owners of most of the violins, there was also certainly a degree of bias in the ratings.

Ideally, a standard for violin quality assessment should be established, including criteria for room acoustics and playing tasks. Quality descriptors should also be standardized. A variation of

the ones used for this thesis could be selected in accordance with [4], with three descriptors + overall quality likely being sufficient. It is important that the players agree on the meaning of the descriptors in order for the ratings to be useful. To that end, it will probably be necessary to train the players how to rate violins. This could be done using representative violins for each descriptor, where the players would have to agree on their sound quality.

With a more robust playing test, it would be interesting to test how much the measured FRF and perceived quality are affected by moving the soundpost or adjusting the bridge, given that this is the most practical way to modify a violin.

Chapter 7 Conclusion

The practical aspects of measuring violin FRFs have been investigated, demonstrating the importance of string damping, excitation method, mass-loading and violin support.

A very simple method has been developed for obtaining admittance and radiativity measurements for the violin bridge using a simple pendulum, both of which can be used to obtain the signature resonances. It has also been shown that a radiativity measurement at the bridge is probably sufficient, since it contains most of the low-frequency information found in bridge admittance measurements. This is a useful step towards making violin analysis more accessible.

While this thesis did not find any link between measurable attributes and perceived quality, it has hopefully served to expand on the knowledge of violin measurement methods, and set the stage for future studies.

Bibliography

- [1] Woodhouse J. "The acoustics of the violin: a review". In: *Rep. Prog. Phys.* 77 (2014).
- [2] Saitis C., Fritz C., Giordano B., and Scavone G. "Bridge admittance measurements of 10 preference-rated violins". In: *Acoustics 2012, Apr 2012, Nantes, France.* (2012).
- [3] Bissinger G. "Structural acoustics of good and bad violins". In: *J. Acoust. Soc. Am.* 124(3) (2008), pp. 1764–1773.
- [4] Fritz C., Blackwell A. F., Cross I., Woodhouse J., and Moore B. C. J. "Exploring violin sound quality: Investigating English timbre descriptors and correlating resynthesized acoustical modifications with perceptual properties". In: *J. Acoust. Soc. Am.* 131(1) (2012), pp. 783–794.
- [5] Flocken H. D. "Can Forced Vibrations Transform the Sound of New Violins?" MA thesis. DTU, 2023.
- [6] Benson N. "Quantitative Assessment of the Impact of Relative Humidity on the Vibro-Elastic Properties of a Violin". MA thesis. DTU, 2024.
- [7] Jansson E.V. "Violin frequency response – bridge mobility and bridge feet distance". In: *Applied Acoustics* 65 (2004), pp. 1195–1205.
- [8] Zhang A. and Woodhouse J. "Reliability of the input admittance of bowed-string instruments measured by the hammer method". In: *J. Acoust. Soc. Am.* 136(6) (2014), pp. 3371–3381.
- [9] Pyrkosz M. and Van Karsen C. "Comparative Modal Tests of a Violin". In: *Experimental techniques. Michigan Technological university. Society for Experimental Mechanics.* (2012).
- [10] Duerinck T., Segers J., Skrodzka E., Verberkmoes G., Leman M., Paepegem W. V., and Kersemans M. "Experimental comparison of various excitation and acquisition techniques for modal analysis of violins". In: *Applied Acoustics* 177 (2021).
- [11] Piacsek A. and Lowery S. "Experimental Uncertainty in Measurements of Violin Impulse Response Admittance". In: *Proceedings of the 10th Convention of the European Acoustics Association Forum Acusticum 2023* (2023), pp. 3423–3428.
- [12] Dünnwald H. "Deduction of objective quality parameters on old and new violins". In: *Catgut Acoust. Soc. J. Vol. 1, No. 7, Series II* (1991), pp. 1–5.
- [13] Brüel & Kjær. *Instructions and Applications. Force Transducer Type 8200.*
- [14] Curtin J. "Measuring Violin Sound Radiation Using an Impact Hammer". In: *J. Violin Soc. Am.: VSA Papers, Vol. XXII, No. 1* (2009), pp. 186–209.
- [15] URL: <https://www.analog.com/media/en/technical-documentation/data-sheets/ADXL345-EP.pdf>.
- [16] URL: <https://www.analog.com/media/en/technical-documentation/data-sheets/MAX4465-MAX4469.pdf>.
- [17] Ren J. and Wang J. "Assessment of transducer mass effects on measured FRFs in shaker modal testing". In: *JVE International LTD. Journal of Vibroengineering, Aug 2017, Vol. 19, Issue 5* (2017), pp. 3472–3487.
- [18] Fritz C., Cross I., Moore B. C. J., and Woodhouse J. "Perceptual thresholds for detecting modifications applied to the acoustical properties of a violin". In: *J. Acoust. Soc. Am.* 122(6) (2007), pp. 3640–3650.
- [19] Woodhouse J. "The Acoustics of "A0-B0" Mode Matching in the Violin". In: *Acta Acustica* 84 (1998), pp. 947–956.

Appendix A Additional Figures

String damping methods



Figure A.1: All string damping methods

Arduino Setup

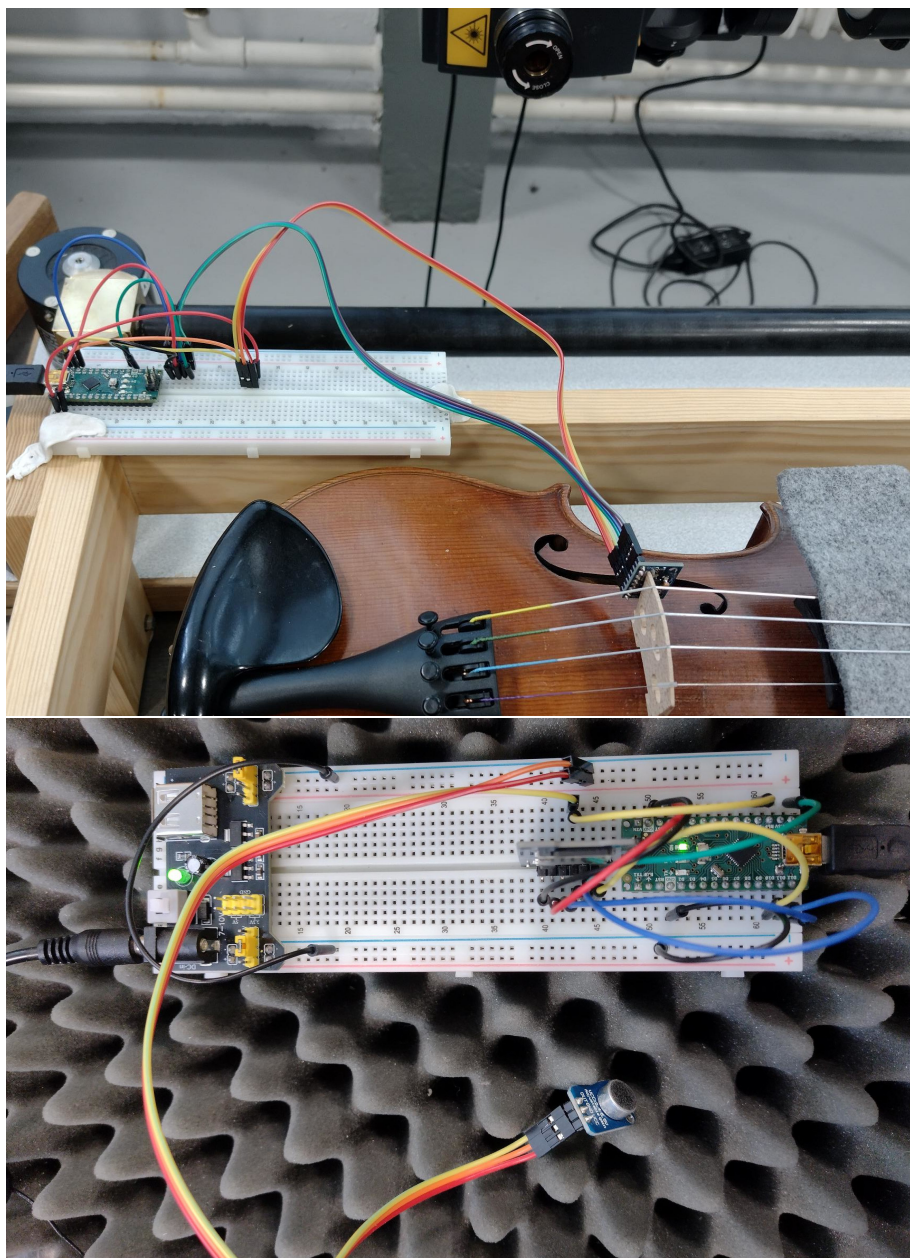


Figure A.2: Top: ADXL345 attached to the bridge. Bottom: Close view of breadboard with MAXX4466.

Mass-Load Admittances

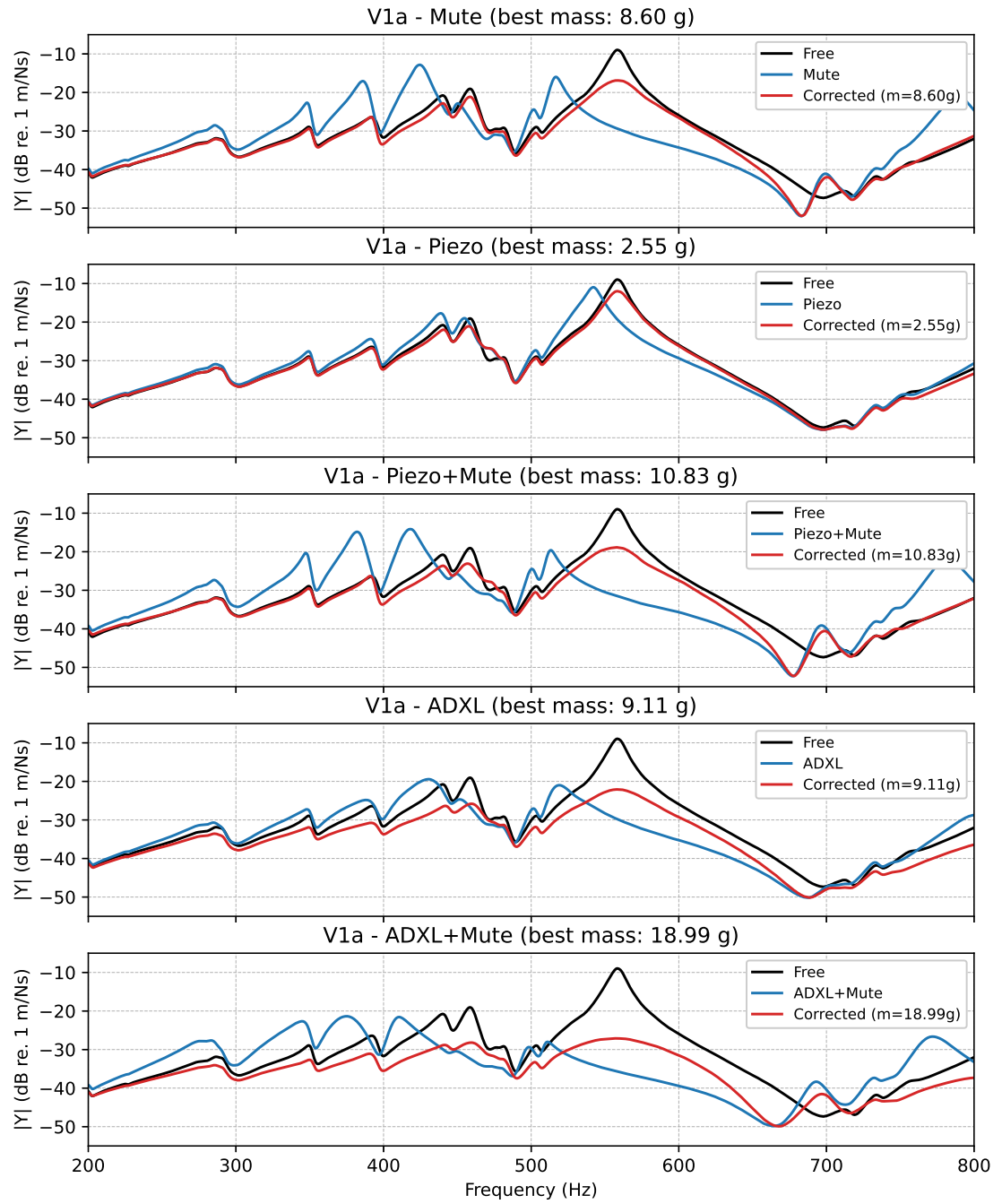


Figure A.3: Free, loaded and corrected bridge admittances for each mass load.

Mass-Load - Best Fit

Mass correction distributions for all sets and loadings

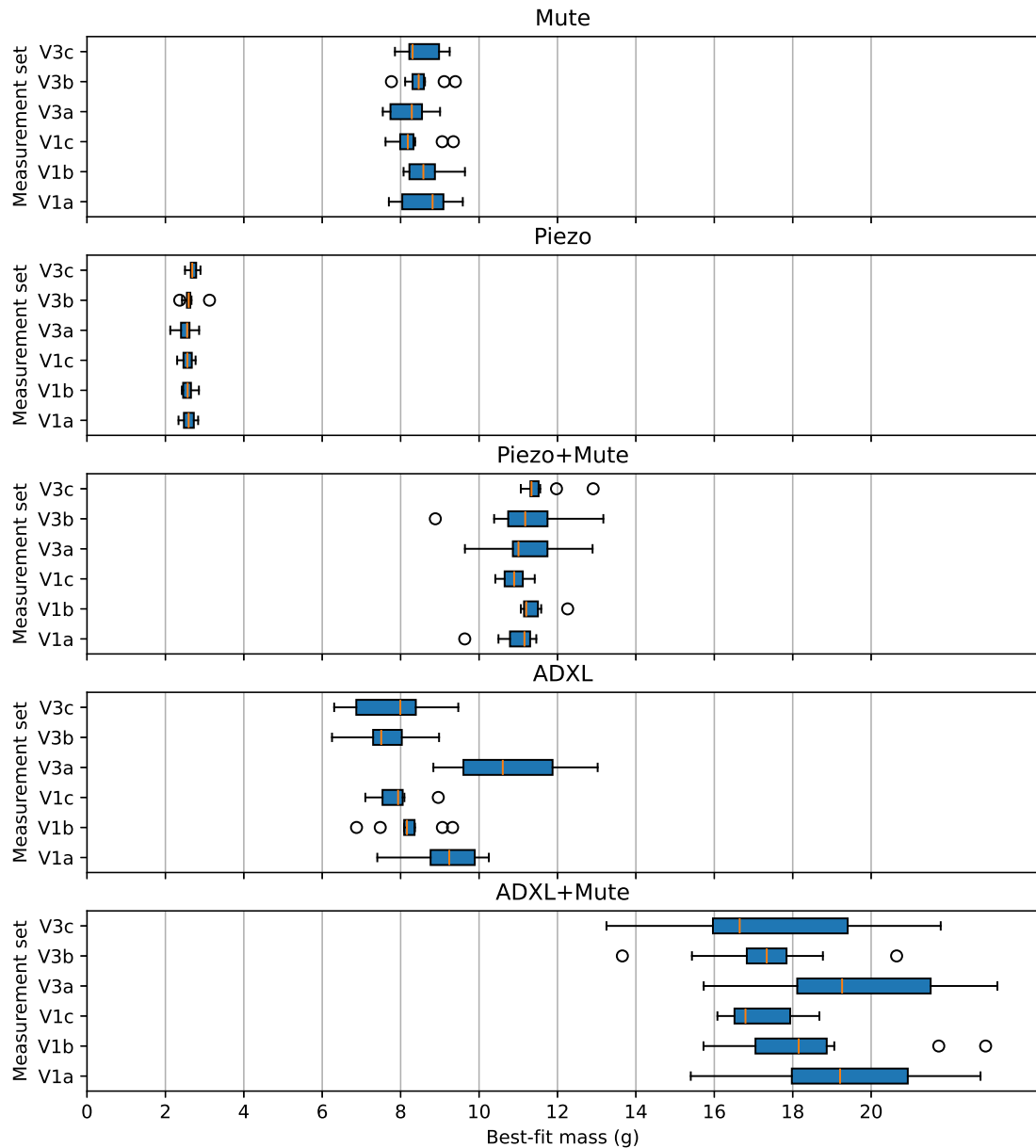


Figure A.4: Boxplots for the best-fit mass-loads for each load type.

Handheld Transducer

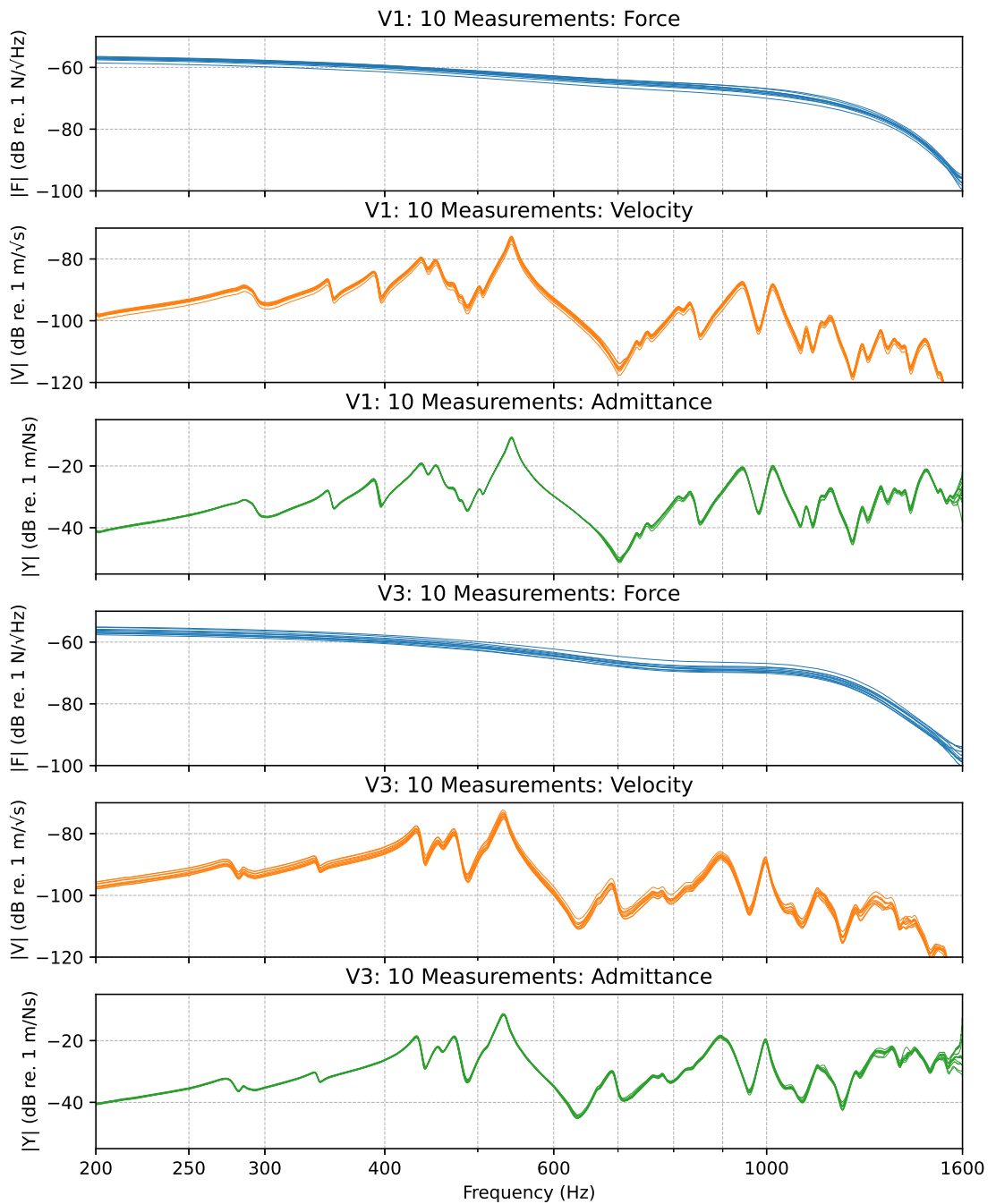


Figure A.5: Impact hammer results for 10 measurements for violins V1 and V3.

Pendulums

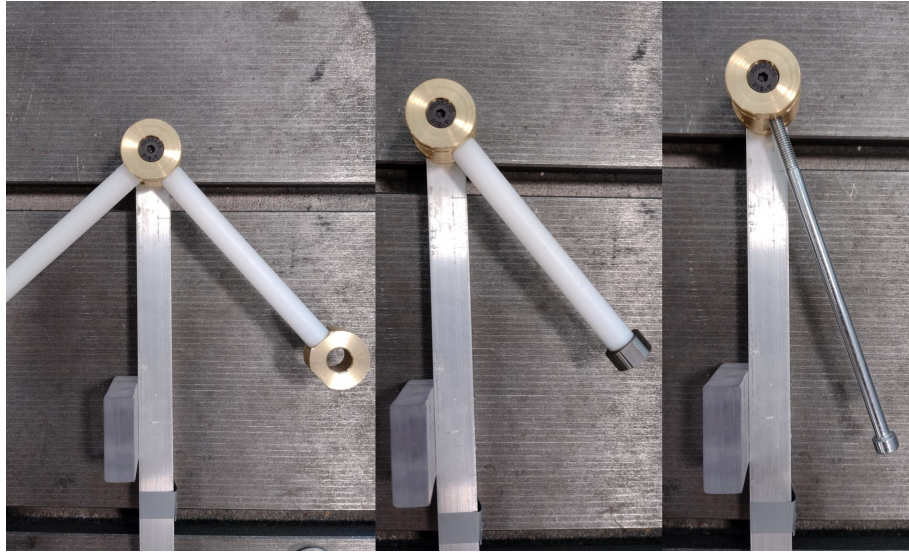


Figure A.6: Left-to-right: Heavy, Middle and Light-Long pendulums. The light-medium and light-short pendulums were just shorter versions of the light-long.

Variances for Force spectrum estimation

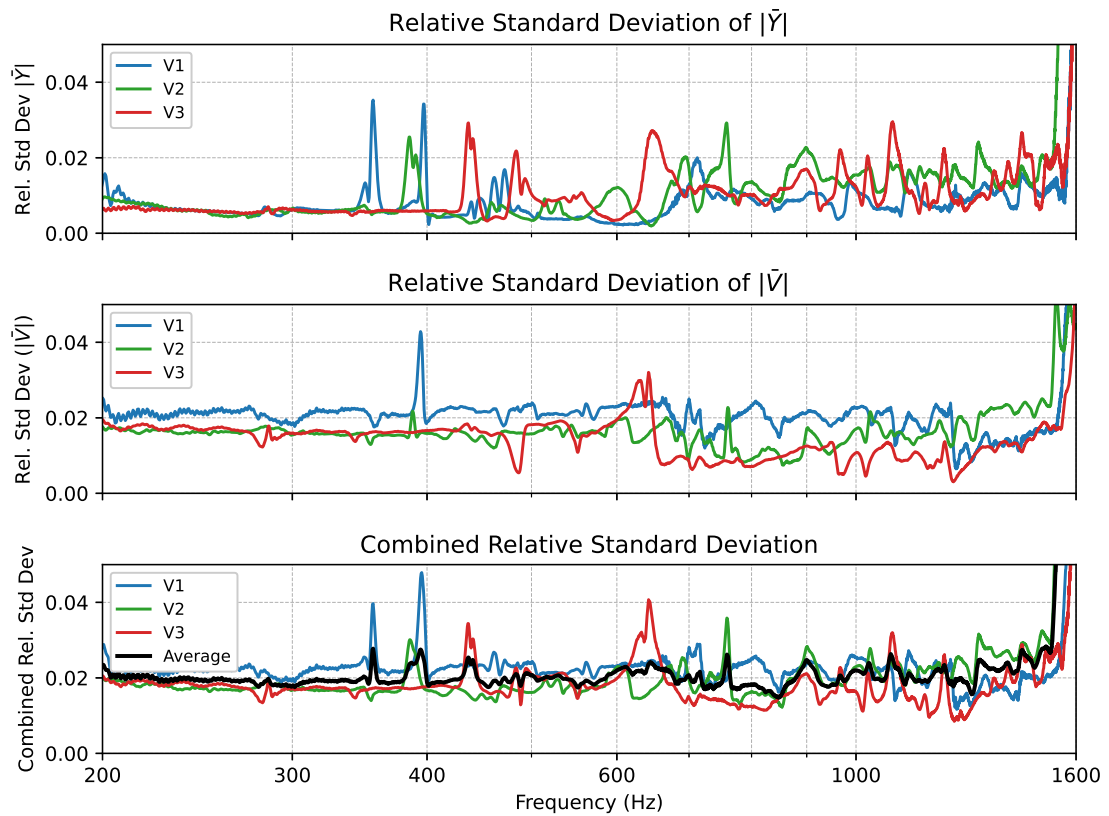


Figure A.7: Separate and combined relative standard deviations.

Final pendulum estimate and total variance

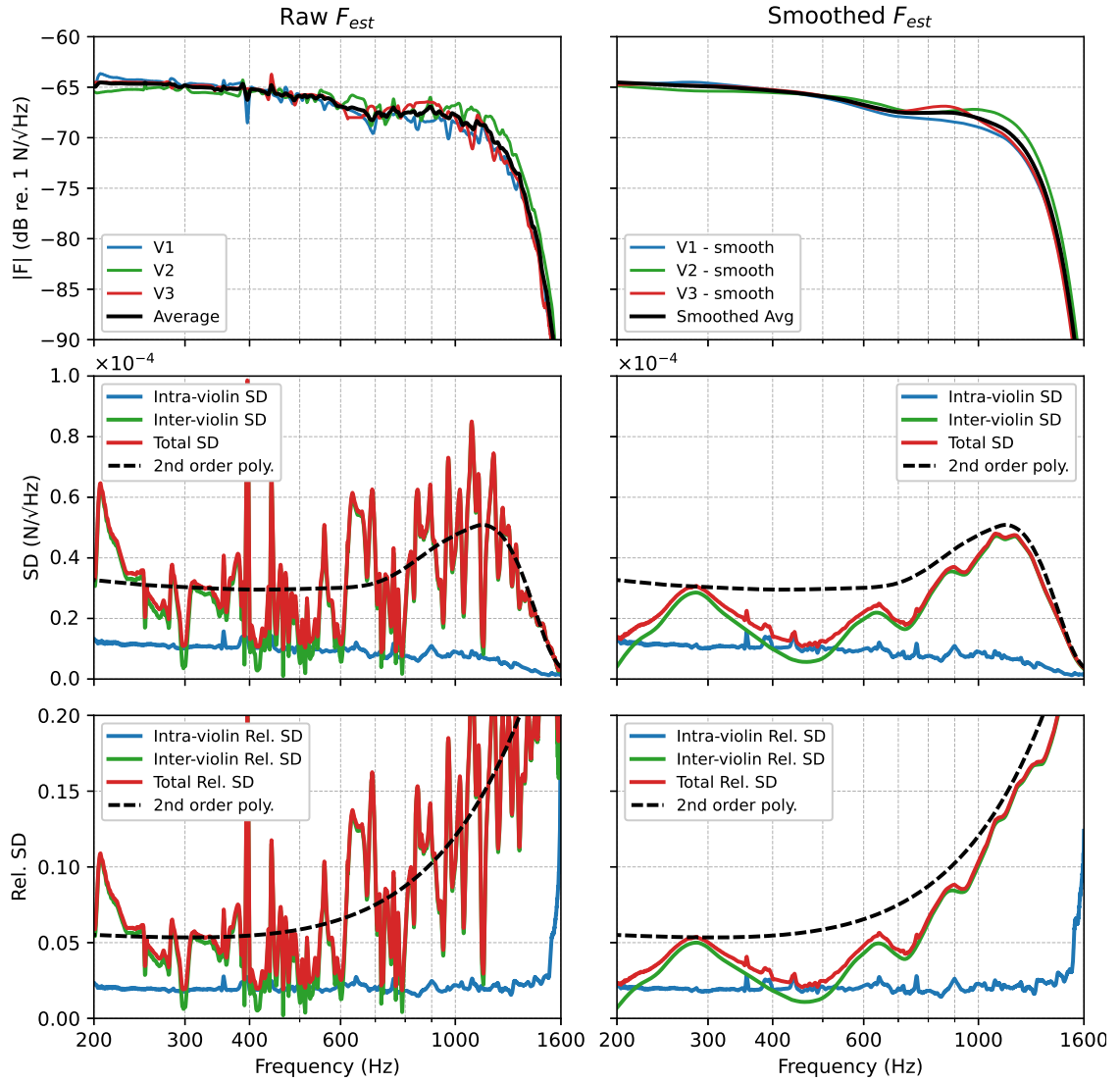


Figure A.8: Estimated pendulum force spectrum and total standard deviation for raw and smoothed results.

Not to scale.
 All lengths in mm.
 65x20 mm pieces of wood.
 All right angles

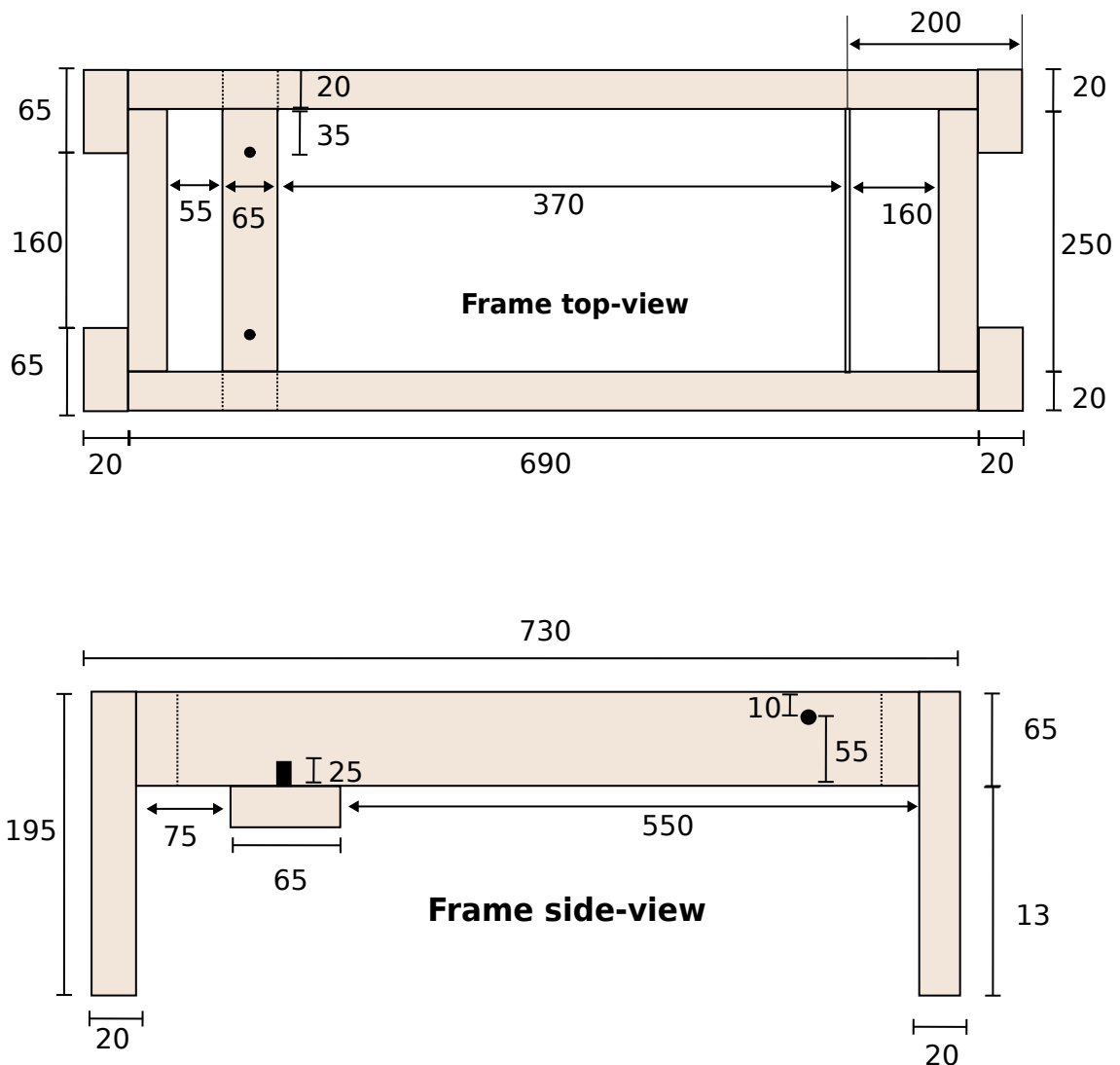


Figure A.9: Drawing of violin frame

Pendulum axis
Material: Brass

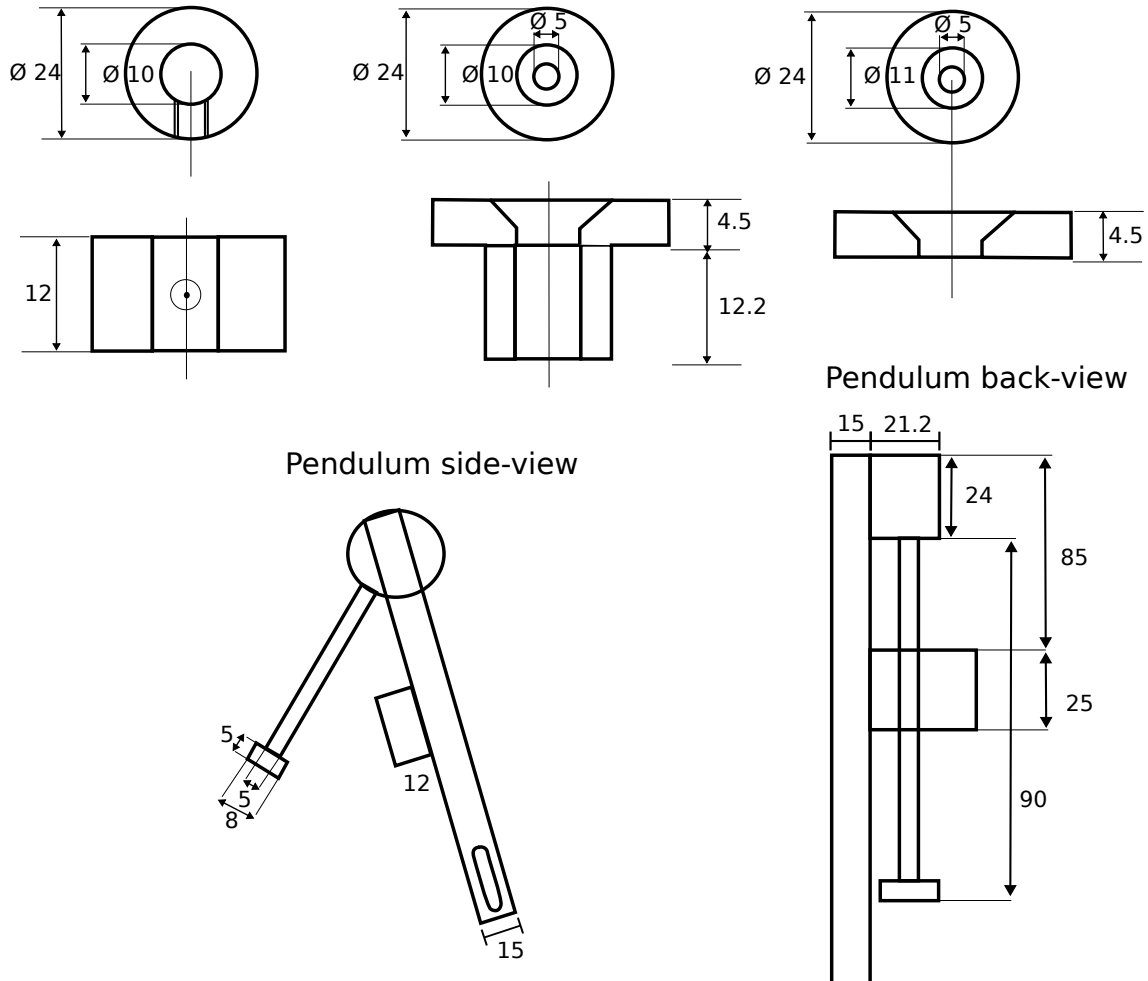


Figure A.10: Pendulum drawings in mm. It should be noted that the author has no prior experience with technical drawings, and that most of the pendulum sizes are estimates due to a lack of access to the lab during the summer.

Appendix B Pendulum Results

Admittance and Radiativity

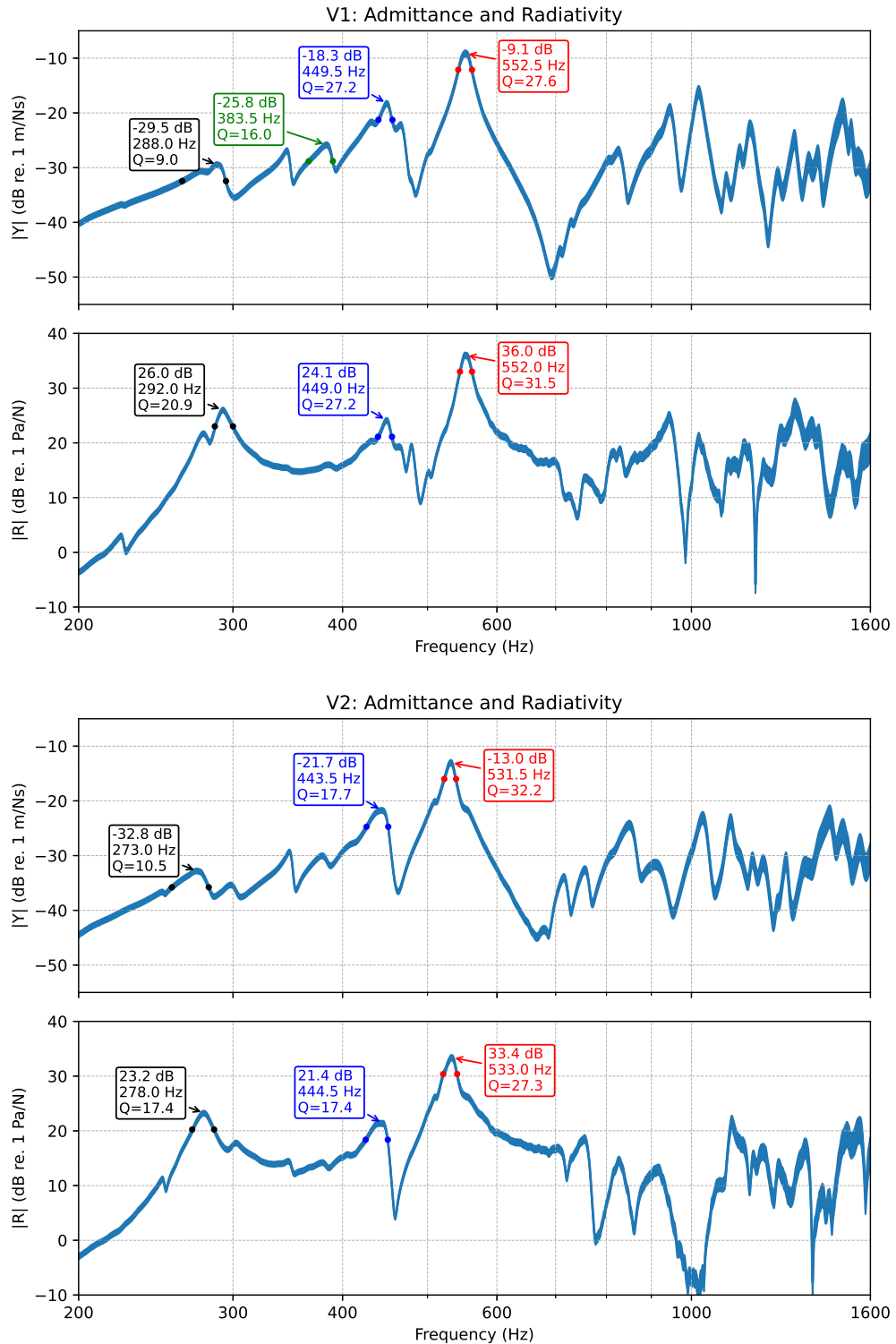


Figure B.1: Violins 1 and 2 annotated with signature resonance information. Shaded area shows the mean admittance/radiativity \pm SE, dots show the 3 dB bandwidth of the resonances.

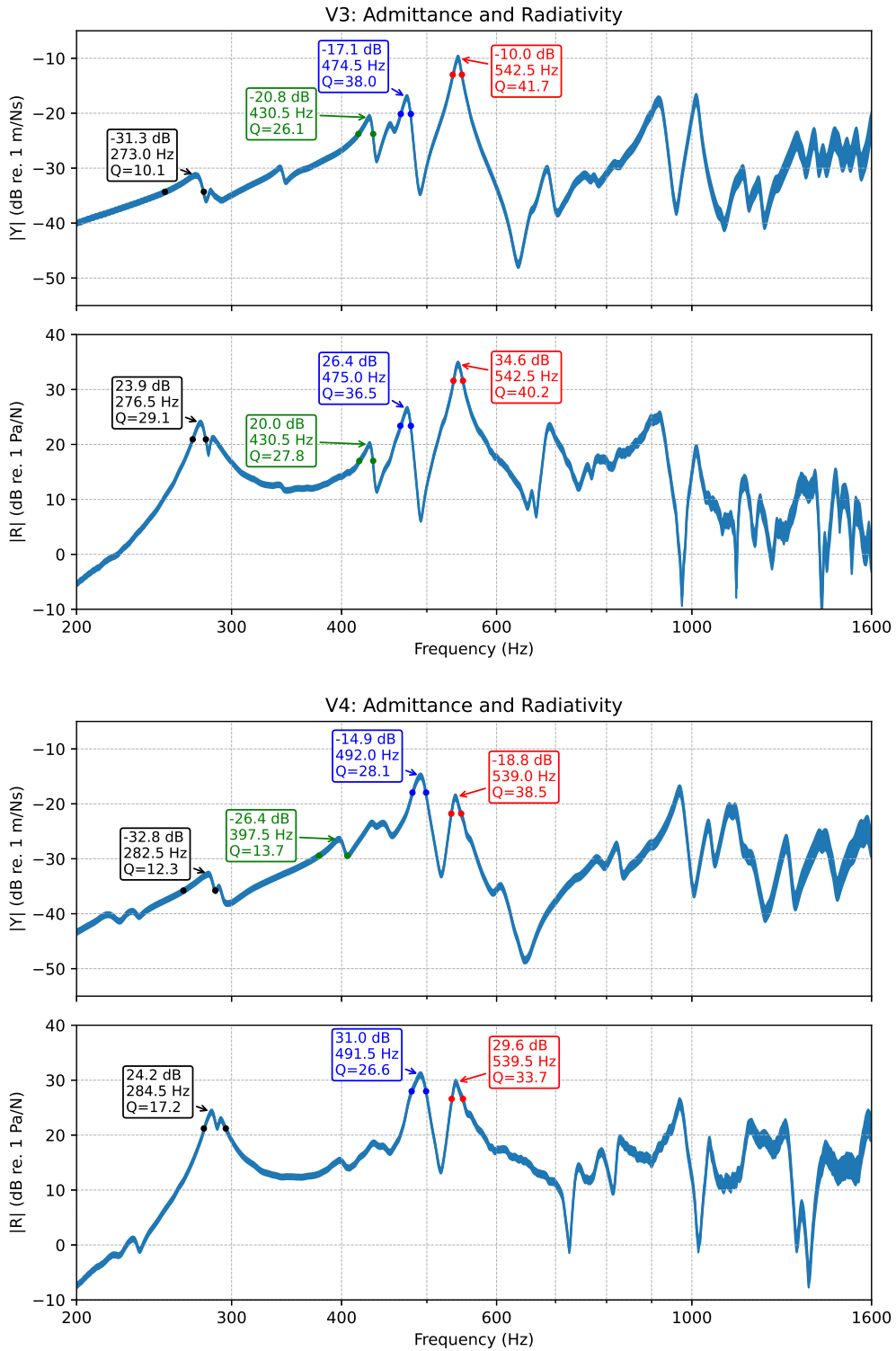


Figure B.2: Violins 3 and 4 annotated with signature resonance information. Shaded area shows the mean admittance/radiativity \pm SE, dots show the 3 dB bandwidth of the resonances.

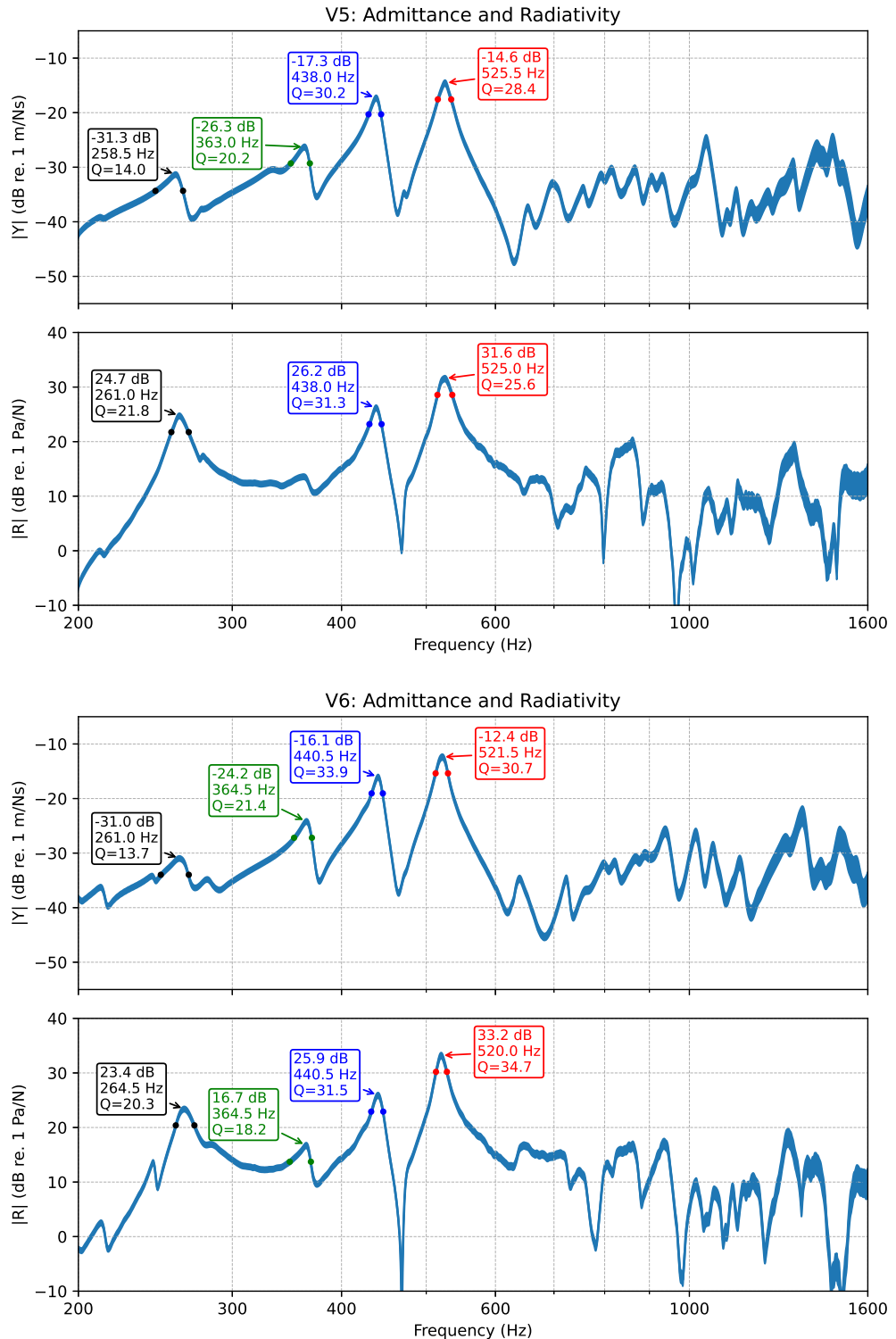


Figure B.3: Violins 5 and 6 annotated with signature resonance information. Shaded area shows the mean admittance/radiativity \pm SE, dots show the 3 dB bandwidth of the resonances.

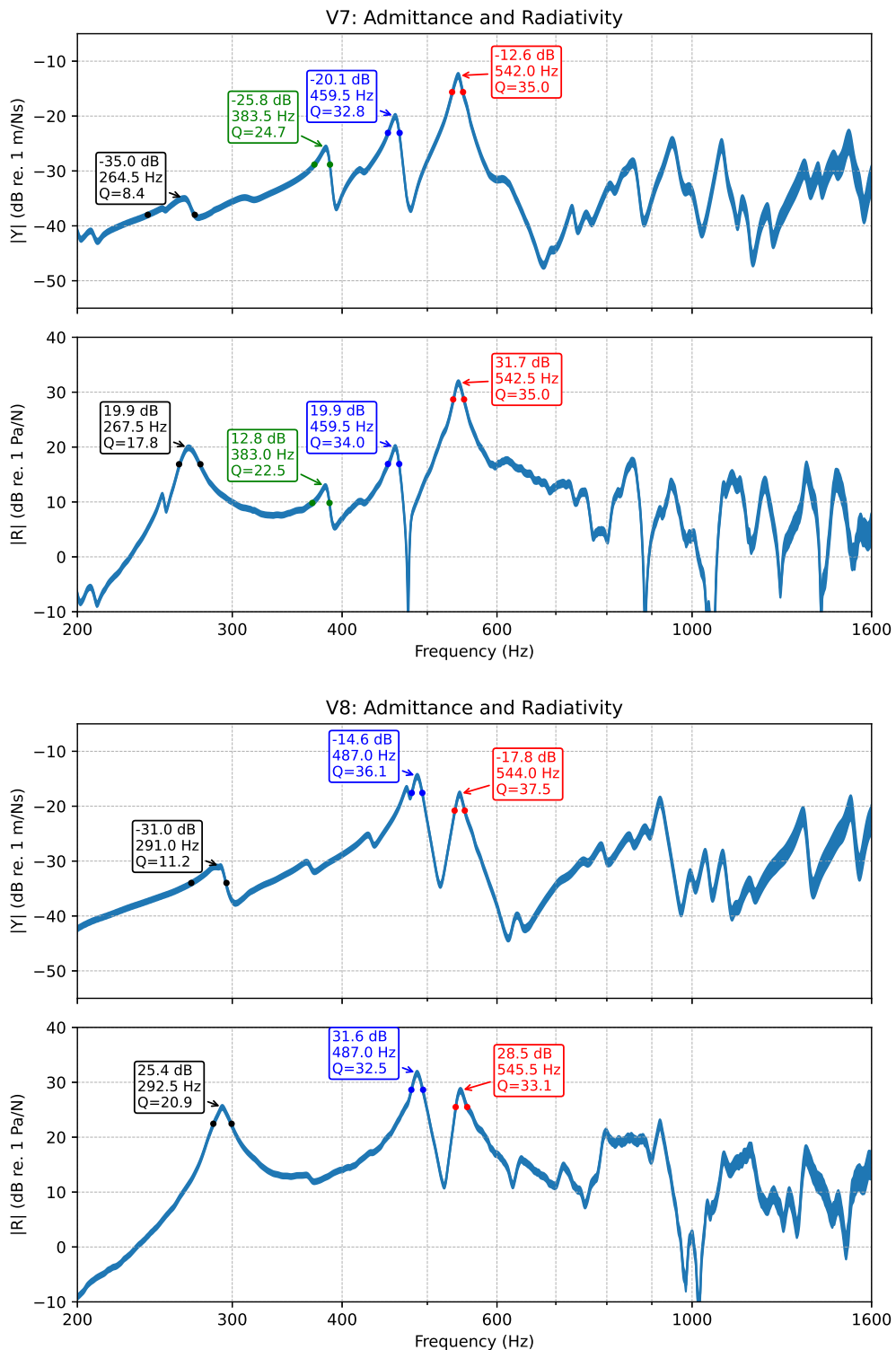


Figure B.4: Violins 7 and 8 annotated with signature resonance information. Shaded area shows the mean admittance/radiativity \pm SE, dots show the 3 dB bandwidth of the resonances.

Quality Assessment

Date: 2025-06-19

Jørgen Skotte

John Hebøll

Table B.1: Quality assessment of violins 1–8. Direct translation from Danish to English.

Violin 1 "Chinese" measurement violin <i>Projection:</i> OK - normal <i>Tone:</i> OK - a bit grainy <i>Balance:</i> OK <i>Comments:</i> An OK playable violin <i>Grade:</i> 8	Violin 5 Jørgen's "youngest" <i>Projection:</i> Large <i>Tone:</i> Bright - clear <i>Balance:</i> OK <i>Comments:</i> Very beautiful tone <i>Grade:</i> 9
Violin 2 "Chinese" reference violin <i>Projection:</i> OK <i>Tone:</i> Lacks fullness. A bit grainy <i>Balance:</i> Powerful on E. Closed on D. <i>Comments:</i> Grainy tone <i>Grade:</i> 7	Violin 6 Jørgen's "middlemost" <i>Projection:</i> Large <i>Tone:</i> Bright - clear <i>Balance:</i> OK <i>Comments:</i> <i>Grade:</i> 9
Violin 3 Holger's violin <i>Projection:</i> OK → large <i>Tone:</i> Sharp - especially on A and E <i>Balance:</i> OK <i>Comments:</i> Resonance on B1 <i>Grade:</i> 7	Violin 7 Jørgen's "oldest" <i>Projection:</i> Quite large <i>Tone:</i> Bright - "middle" <i>Balance:</i> A-string, B-resonance. <i>Comments:</i> <i>Grade:</i> 8
Violin 4 John's violin <i>Projection:</i> Large <i>Tone:</i> A bit dark - closed <i>Balance:</i> OK <i>Comments:</i> <i>Grade:</i> 8	Violin 8 John's family violin <i>Projection:</i> OK - a bit weak on G and D <i>Tone:</i> A bit raspy <i>Balance:</i> A bit weak bass <i>Comments:</i> OK violin. 140-160 years old. <i>Grade:</i> 7

But of bliss and glad life there is little to be said, before it ends; as works fair and wonderful, while they still endure for eyes to see, are ever their own record, and only when they are in peril or broken for ever do they pass into song. - J.R.R. Tolkien

Technical
University of
Denmark

Ørsteds Plads, Building 352
2800 Kgs. Lyngby
Tlf. 4525 1700

www.electro.dtu.dk